

Faculty of Science and Engineering
Department of Petroleum Engineering

**Effect of Organic Surface Concentration on CO₂-Wettability of
Reservoir Rock**

Muhammad Ali

**This thesis is presented for the Degree of
Master of Philosophy (Petroleum Engineering)
of
Curtin University**


January 2018

DECLARATION OF ACADEMIC INTEGRITY

To the best of my knowledge and belief this thesis contains no material previously published by any other person except where due acknowledgment has been made.

This thesis contains no material which has been accepted for the award of any other degree or diploma in any university.

Name: Muhammad Ali

Signature:  _____

Date: January 25, 2018

DEDICATION

I would like to dedicate my thesis to my father, Muhammad Anwar Sahito, who has been my biggest motivation throughout my education; to my mother, Gulnar, for her prayers; to my wife, Roohina Alisha Almas Ali, for her support; and to my lovely daughter Aafreen Noor Sahito.

ACKNOWLEDGMENT

In The Name of Allah, The Most Gracious, The Most Merciful

Firstly, I would like to express my utmost sincere appreciation to my supervisor Dr Stefan Iglauer. I am grateful for his continual guidance and knowledge, which have provided the energy for me to push through the difficulties during my MS research.

Besides my advisor, I would like to thank the rest of my thesis committee, Dr Mofazzal Hossain, Dr Ahmed Barifcani, Dr Mohammad Sarmadivaleh and Dr Linda Stalker, for their insightful comments and encouragement, but also for the hard questions, which incentivised me to widen my research from various perspectives.

My sincere thanks also go to Mr Bob Webb, who provided me with help in all aspects of my experimental work, and who gave access to the laboratory and research facilities. Without his precious support, it would not have been possible to conduct this research.

I thank my fellow colleagues and friends for the stimulating discussions, the sleepless nights we spent working together before deadlines, and all the fun that we have had in the last two years. In particular, I am grateful to Dr Muhammad Arif and Dr Sarmad Al-Anssari for enlightening me with my first glance of research.

I also acknowledges the support provided from the Australian Government (Research Training Program formerly Research Training Scheme) as well as Curtin University for providing the Curtin University Postgraduate Scholarship for this research studies.

Last but not the least, I would like to thank my family—my parents, brothers and sisters—for supporting me spiritually throughout the writing of this thesis and my life in general.

ABSTRACT

Geo-sequestration of carbon dioxide involves injection and subsequent storage of CO₂ in a porous geologic medium. There are certain petro-physical parameters that influence CO₂ flow behaviour and distribution in the reservoir, and these in turn affect trapping capacities. From this perspective, one important physicochemical parameter is the wettability of rock/CO₂/brine, which explains the interfacial interaction between the rock and CO₂. There have been several studies that have characterised the wettability of rock/CO₂/brine systems for proxy minerals such as mica, quartz and calcite, and for composite samples such as shales and coals. However, one important aspect which has not been considered in earlier wettability studies is the organic concentration present in the deep saline aquifers and depleted hydrocarbon reservoirs. Therefore, this study focuses on the effect of organic concentrations on the wettability of rock-forming minerals. Advancing and receding contact angles were measured in typical reservoir conditions (10 MPa, 25 MPa, 323 K) on samples aged (aging time 7 days, atmospheric conditions) in organic acids for a duration sufficient to mimic subsurface behaviour. The minerals chosen for this study included calcite and quartz, and the organic acids chosen were hexanoic acid (C6), lauric acid (C12), stearic acid (C18), and lignoceric acid (C24). The selected organic acids varied in terms of the number of carbon atoms, ranging from six to 24. The results showed that the CO₂/brine/mineral contact angle increased with the presence of organic acids, implying that quartz and calcite reservoir minerals progressively transform from water-wet to CO₂-wet conditions. In addition, the contact angles were higher when the mineral samples were aged in organic acids with a higher number of carbon atoms in their molecular chain. The results of the study led to an improved understanding of the phenomena at the brine/mineral interface during CO₂ geo-sequestration in the presence of organic acids.

PUBLICATIONS

Publications as part of thesis

Ali M., Arif, M., Al-Anssari, S., Linda, S., Sarmadivaleh, M., Barifcani, A., Iglauer, S., (2018), CO₂-wettability of sandstones under the influence of organic acids: implications for CO₂ trapping/storage, *Geochimica et Cosmochimica Acta*, under review.

Ali M., Arif, M., Al-Anssari, S., Linda, S., Sarmadivaleh, M., Lebedev, M., Barifcani, A., Iglauer, S., (2017), Organic acid concentration thresholds for aging of carbonate minerals: implications for CO₂ trapping/storage, *Earth and Planetary Science Letters*, under review.

Publications as not part of thesis

Ali, M., Al-Anssari, S., Shakeel, M., Arif, M., Dahraj, N. U., & Iglauer, S. (2017, October). Influence of Miscible CO₂ Flooding on Wettability and Asphaltene Precipitation in Indiana Lime Stone. *In SPE/IATMI Asia Pacific Oil & Gas Conference and Exhibition. Society of Petroleum Engineers.*

Al-Anssari, S., Nwideo, L., **Ali, M.**, Sangwai, J. S., Wang, S., Barifcani, A., & Iglauer, S. (2017, October). Retention of Silica Nanoparticles in Limestone Porous Media. *In SPE/IATMI Asia Pacific Oil & Gas Conference and Exhibition. Society of Petroleum Engineers.*

Dahraj, N. U., **Ali, M.**, & Khan, M. N. (2016, November). End of Linear Flow Time Picking in Long Transient Hydraulically Fractured Wells to Correctly Estimate the Permeability, Fracture Half-Length and Original Gas in Place in Liquid Rich Shales. *In PAPG/SPE Pakistan Section Annual Technical Conference and Exhibition. Society of Petroleum Engineers.*

Contents

DECLARATION OF ACADEMIC INTEGRITY.....	I
DEDICATION	II
ACKNOWLEDGMENT	III
ABSTRACT.....	IV
PUBLICATIONS	V
Publications as part of thesis.....	V
Publications as not part of thesis.....	V
Contents	VI
List of Figures	IX
List of Tables	XI
Chapter 1 Overview and thesis objectives.....	1
1.1 Background	1
1.2 Motivation of the thesis.....	3
1.3 Objectives of thesis.....	4
1.4 Organisation of thesis	5
Chapter 2 Literature review	7
2.1 Introduction	7
2.2 CO ₂ phase behaviour	7
2.3 Carbon capture and storage.....	8
2.3.1 Underground storage options	10
2.3.2 Trapping mechanisms	12
2.3.2.1 Structural trapping	12
2.3.2.2 Capillary or residual trapping.....	13
2.3.2.3 Solubility trapping	14
2.3.2.4 Mineral trapping	14
2.4 Introduction to rock/fluid wettability.....	15
2.4.1 Contact angle method	16
2.4.2 Advancing and receding angles.....	17
2.4.3 Impact of wettability on structural and residual trapping	18
2.4.4 Previous studies on CO ₂ wettability	19
2.4.4.1 Pure minerals.....	19

2.4.4.2	Wettability of altered surfaces.....	21
2.5	Fatty acids in sediments	22
2.6	Influence of organic acids on rock wettability	22
2.7	Other factors influencing wettability	25
Chapter 3	Materials and Methods.....	27
3.1	Introduction	27
3.2	Materials.....	27
3.2.1	Fluids and Salts.....	27
3.2.2	Organic acids.....	28
3.2.3	Minerals used	29
3.2.4	Cleaning agents	29
3.3	Surface roughness.....	29
3.4	Ageing procedure	29
3.5	Contact angle measurements	30
3.5.1	Contact angle measurements setup.....	31
3.5.2	Imaging procedure.....	35
3.6	Summary of operating conditions.....	35
3.6.1	Calcite	36
3.6.2	Quartz.....	36
Chapter 4	Results and Discussion.....	37
4.1	Introduction	37
4.2	Calcite Results	37
4.2.1	Surface roughness measurements.....	38
4.2.2	Contact angle measurements.....	39
4.2.2.1	Effect of stearic acid concentration	39
4.2.2.2	Effect of pressure on calcite/CO ₂ /brine contact angles	42
4.2.2.3	Comparison with natural calcite.....	43
4.2.2.4	SEM/EDS analysis of calcite surfaces.....	44
4.3	Quartz Results	45
4.3.1	Contact angle measurements.....	45
4.3.1.1	AFM measurements.....	45
4.3.1.2	Influence of organic acids on quartz wettability	45
4.3.1.3	Influence of type of organic acid on quartz	50

4.3.1.4	SEM of quartz	52
4.3.1.5	Comparison of quartz and calcite	53
4.3.1.6	Influence of pressure.....	55
Chapter 5	Conclusions and Recommendations.....	56
5.1	Conclusion.....	56
5.2	Recommendations.....	57
	References.....	58
	Appendix.....	71

List of Figures

Figure 1-1-1 Thesis layout	6
Figure 2-1 CO ₂ phase diagram (after King and Bott, 2012).	8
Figure 2-2 A stepwise illustration of the carbon capture and storage procedure (after CO ₂ CRC web data).	9
Figure 2-3 Geological CO ₂ sequestration options. Extreme left: enhanced oil recovery with CO ₂ flooding; centre left: storage in deep saline aquifer; centre right: storage in depleted hydrocarbon reservoirs; extreme right: storage in coal seams (modified after GRREBS web data).	11
Figure 2-4 Types of structural traps: a) anticline structural trap; b) normal fault trap c) stratigraphic fault structural trap; d) thrust trap structural trap (source: modified after Fundamentals of Petroleum Engineering, module 2, slidershare.net).	13
Figure 2-5 CO ₂ trapping mechanisms' performance over time (after IPCC, 2005)..	14
Figure 2-6 Illustration of trapping mechanisms (after Burnside & Naylor, 2011)....	15
Figure 2-7 Water droplet under interfacial forces in a solid/air/brine system.....	17
Figure 2-8 Illustration of advancing and receding contacting angles (after Yanez-Soto et al., 2015).	18
Figure 2-9 Contact angle data for mineral/CO ₂ /brine systems (modified after Iglauer, 2017).	21
Figure 3-1 Schematic representation of experimental setup used to measure advancing and receding contact angles (modified after Arif et al., 2017a). (a) CO ₂ supply; (b) ISCO (high precision syringe pump) for CO ₂ ; (c) ISCO (high precision syringe pump) for brine; (d) high pressure mixing reactor for fluid equilibration; (e) high pressure cell (inside visible with substrate retained on a tilted plate); (f) heating unit and controller for high pressure cell; (g) liquid drain system; (h) high resolution video camera; (i) desktop computer installed with image visualisation and interpretation software; (j) gas pressure relief valve (modified after Arif et al., 2017a).	32
Figure 3-2 Example images extracted from video files for contact angle measurements. Figure (a) and (b) are taken at 10 ⁻² M of stearic acid on a calcite surface at 10 MPa and 25 MPa; Figure (c) and (d) are taken at 10 ⁻² M of hexanoic acid and stearic acid respectively on a quartz surface at 25 MPa; all were taken at 323 K; CO ₂ is in surrounding	34
Figure 3-3 Schematic of contact angle measurements. Right (blue) is 'receding angle', and left (red) is 'advancing angle' (modified after Arif et al., 2017a).....	35

Figure 4-1 Calcite/CO₂/brine contact angles measured as a function of stearic acid concentration at 323 K, and at 10 MPa and 25 MPa; C_{stearic} is the stearic acid concentration (molarity). The green dotted line represents the structural trapping limit, while the blue dotted line represents the optimal capillary trapping limit. The zone above the green dotted line indicates the reduced CO₂ zone. 41

Figure 4-2 (Reaction Scheme) Chemisorption of stearic acid (CH₃(CH₂)₁₆-COOH) on solid calcite surface (∧ indicates solid bulk) (sources: Cao et al., 2016; Heberling et al., 2011; Mihajlović et al., 2013; Shi et al., 2010; Wang et al., 2006). 43

Figure 4-3 Quartz/CO₂/brine contact angles as a function of hexanoic acid concentration; C_{hexanoic} is the hexanoic acid concentration (molarity). Solid lines: advancing; dotted lines: receding. Red: ambient pressure; green: 25 MPa. 47

Figure 4-4 Quartz/CO₂/brine contact angles as a function of lauric acid concentration; C_{lauric} is the lauric acid concentration (molarity). Solid lines: advancing; dotted lines: receding. Red: ambient pressure; green: 25 MPa. 48

Figure 4-5 Quartz/CO₂/brine contact angles as a function of stearic acid concentration; C_{stearic} is the stearic acid concentration (molarity). Solid lines: advancing; dotted lines: receding. Red: ambient pressure; green: 25 MPa. 49

Figure 4-6 Quartz/CO₂/brine contact angles as a function of lignoceric acid concentration; C_{lignoceric} is the lignoceric acid concentration (molarity). Solid lines: advancing; dotted lines: receding. Red: ambient pressure; green: 25 MPa. 49

Figure 4-7 Quartz/CO₂/brine contact angles as a function of different organic acid concentration at 25 MPa and 323 K; C_{organic} is the different organic acid concentration (molarity). Dotted blue horizontal lines in the graph define the threshold of capillary trapping ($\theta = 50^\circ$), and Dotted green horizontal lines in graph define the threshold for structural trapping ($\theta > 90^\circ$). 51

Figure 4-8 Quartz vs. calcite wettability (aged in stearic acid at 25 MPa and 323 K) C_{stearic} is the stearic acid concentration (molarity). 54

Figure 4-9 (Reaction Scheme) Chemisorption of different organic acids on solid quartz surface (∧ indicates solid bulk). 55

List of Tables

Table 2-1 Worldwide CO ₂ storage projects (modified after IPCC, 2005).....	10
Table 2-2 Storage capacity estimates and relative merits of storage mediums (after IPCC, 2005).....	11
Table 2-3 Wettability regimes for rock/CO ₂ /brine systems on the basis of contact angle (modified after Iglauer et al., 2015a).	17
Table 2-4 Previous wettability studies which considered organic acids.....	23
Table 3-1 Fluids used in this study.	27
Table 3-2 Classification of organic acids.	28
Table 3-3 Organic acids used in this study.	28
Table 4-1 Surface roughness of calcite surfaces before and after ageing in stearic acid	38
Table 4-2 Contact angle measurements at different stearic acid concentrations.....	41
Table 4-3 SEM/EDS composition analysis of calcite surfaces	44
Table 4-4 Contact angle measurements at different concentrations of different organic acids at (0.1 MPa and 323 K)	46
Table 4-5 Contact angle measurements at different concentrations of different organic acids at (25 MPa and 323 K)	46
Table 4-6 SEM/EDS of quartz surfaces aged in hexanoic acid.....	52
Table 4-7 SEM/EDS of quartz surfaces aged in lauric acid.....	52
Table 4-8 SEM/EDS of quartz surfaces aged in stearic acid	53
Table 4-9 SEM/EDS of quartz surfaces aged in lignoceric acid	53

Chapter 1 Overview and thesis objectives

1.1 Background

Carbon dioxide (CO₂) is a significant component of greenhouse gas emissions (Change, 2007; Fiala, 2009), which are the principal contributors to the global warming that is causing a significant rise in the earth's temperature (Davis et al., 2010; Karl, 2009; Solomon et al., 2009). According to a joint report by the National Aeronautics and Space Administration and the National Oceanic and Atmospheric Administration, the global temperature in 2015 was 1.78 °F (0.99 °C) warmer than the mean global temperature of the mid-20th century (NASA and NOAA, 2016). This poses a direct threat to human life.

CO₂ concentrations have risen significantly over the last two centuries, with a level of 401.5 ppm in 2017 compared to 280 ppm in 1750 (Cape Grim, 2017; Davis et al., 2016; Nordhaus, 2014). There are many approaches being undertaken to mitigate CO₂ emissions, including carbon-free wind power, carbon-free solar panels, and underground geological storage (Chu & Majumdar, 2012; Herrero et al., 2016; Hristov et al., 2013; Lackner, 2003; Schiermeier et al., 2008). Of these strategies, geological CO₂ storage has proven to be a very promising approach to controlling anthropogenic emissions (Kelemen & Matter, 2008; Lackner, 2003). This technology is known broadly as carbon capture and storage (CCS).

In CCS, CO₂ is first captured at major point sources, such as fossil fuel power plants, and then transmitted to a storage site and injected into depleted hydrocarbon reservoirs or deep saline aquifers (Holloway, 2007; Rackley, 2009). The geological storage formation provides a safe storage medium for long-term trapping and immobilisation of CO₂. After the commencement of CO₂ injection into the reservoirs or aquifers, trapping mechanisms render CO₂ immobile in the porous medium. These trapping mechanisms include structural trapping (Arif et al., 2016a, b, 2017a; Iglauer et al., 2015a), capillary or residual trapping (Iglauer et al., 2011a, b; Juanes et al., 2010; Krevor et al., 2012; Pentland et al., 2011), mineral trapping (Golding et al., 2011; Pearce et al., 2015), and dissolution trapping (Agartan et al., 2015; Iglauer, 2011c).

Another mechanism is adsorption trapping of CO₂, which is the dominant gas storage mechanism in coal seams and organic rich shales (Arif et al., 2016c, 2017).

Structural and residual trapping capacities are the most significant trapping methods, especially during the first decade of a storage project. Among other reservoir and geochemical factors, the wettability of CO₂/brine/rock systems is the most fundamental physicochemical parameter, and is significantly related to the structural and residual trapping capacities (Arif et al., 2016d; El-Maghraby and Blunt, 2012; Iglauer et al., 2015a, b; Spiterei et al., 2008). If the rock/CO₂/brine system is strongly water-wet, then structural and residual trapping potential is higher; for CO₂-wet systems, the trapping potential is significantly reduced. Hypothetically, in scenarios where the caprock is CO₂-wet, the capillary forces outbalance the buoyancy force, resulting in capillary breakthrough of CO₂ through the caprock. This phenomenon has been shown to reduce structural and residual trapping capabilities significantly. More specifically, laboratory core-flooding studies, micro-CT 3D imaging of cores saturated with brine and CO₂, and numerical simulation models, have shown that trapping potential is higher in situations when rock is water-wet (Chaudhary et al., 2013; Iglauer et al., 2015a, b; Krevor et al., 2015).

Generally, the wettability of CO₂/brine/mineral systems is characterised by experimental measurement of the advancing and receding contact angles (Broseta et al., 2012; Chiquet et al., 2007; Lander et al., 1993; ShojaiKaveh et al., 2012; Wan et al., 2014). The other methods to assess the wetting behaviour of rock/fluid systems include the Amott Harvey Index (Amott, 1959) and the USBM method (Donaldson et al., 1969). In addition, capillary pressure and relative permeability curves provide qualitative insight into the wetting characteristics of rock/fluid systems (Bryant and Blunt, 1992; Spiteri et al., 2008). Many studies have comprehensively reported the wettability of various naturally occurring minerals, such as pure calcite (Arif et al., 2017a; Broseta et al., 2007; Farokhpour et al., 2013), pure quartz (Saraji et al., 2013; Sarmadivaleh et al., 2015), mica (Arif et al., 2016a; Farokhpour et al., 2013; Wan et al., 2014), coals (Arif et al., 2016c; ShojaiKaveh et al., 2011), and shales (Arif et al., 2017b; Iglauer et al., 2015b; Roshan et al., 2016; ShojaiKaveh et al., 2016). The factors responsible for altering wettability, as a function of temperature, pressure and salinity, have also been highlighted (Arif et al., 2017c, d, e). Such wettability data combined

with CO₂/brine interfacial tension provides a quantitative assessment of the structural trapping potential.

Reservoirs and aquifers contain noticeable amounts of naturally existing organics, ranging from short chain to long chain acids (Barth, 1991). Specific examples include acetic acid (C2), hexanoic acid (C6), lauric acid (C12), stearic acid (C18), and lignoceric acid (C24); the number of carbon atoms in these acids ranges from two to 24 (Feng et al., 2007; Grabowski et al., 2005; Seewald, 2003). However, the presence of these organics in the system has not been considered by previous wettability studies. Such organics have been shown to have a considerable effect on the fluid flow distribution and, consequently, the wetting behaviour. Therefore, investigation of CO₂/brine/mineral wettability in the presence of organics, and in relevant subsurface conditions, is required to depict true wetting behaviour. Such predictions would lead to realistic assessment of the trapping potential, resulting in reduced uncertainty associated with CO₂ storage.

1.2 Motivation of the thesis

Previous studies have described classifications of rock wetting characteristics, varying from strongly water-wet to strongly CO₂-wet (Iglauer et al., 2015a; Iglauer, 2017). Experimental and numerical studies have proven that CO₂-wet surfaces radically reduce structural (Arif et al., 2016d, 2017a; Iglauer et al., 2015b) and capillary trapping capacities (Al-Khdheawi et al., 2017a, b; Al-Menhali et al., 2016; Chaudhary et al., 2013; Rahman et al., 2016). In this context, it is clear that the organic content of the rock surface plays a vital role in causing a mineral surface that is initially water-wet to become CO₂-wet (Arif et al., 2017b; Iglauer et al., 2015b, 2017). For example, several important rock-forming mineral surfaces, such as calcite, quartz and mica, are strongly water-wet or weakly water-wet (Al-Anssari et al., 2017a; Arif et al., 2016a, b; Broseta et al., 2012; Chiquet et al., 2007). In contrast, naturally occurring high-TOC shales, coals or alkylated or styrolated minerals, and minerals aged in crude oil (Arif et al., 2017b; Dickson et al., 2006; Iglauer, 2017; Yang et al., 2007), are weakly, strongly or even completely CO₂-wet; the extent depends on the operating pressure, temperature and brine composition (Chen et al., 2015; Iglauer et al., 2012).

However, chemically clean mineral surfaces are artificial, in that they can only be prepared and persist in strongly oxidising environments (Iglauer et al., 2014; Love et al., 2005). Moreover, it is well established that anoxic or reducing conditions prevail in the subsurface, i.e. the environment becomes more reducing with increasing depth (Froelich et al., 1979; Townsend et al., 2003). In addition, there is evidence that storage formations always contain traces of dissolved organic material, for example in field-scale pilot-tests (Kharaka et al., 2009) and laboratory studies (Jardine et al., 1989; Madsen and Ida, 1998; Stalker et al., 2013; Yang et al., 2015). A partial monolayer of small traces adsorbed on the mineral surface has the potential to cause a total wettability reversal of the system, from strongly water-wet to completely non-wetting (Adamson & Gast, 1997; Hansen et al., 2000; Iglauer et al., 2014). Consequently, in the case of CO₂/brine/mineral systems, the anticipated water-wet system may eventually be CO₂-wet, implying that the structural trapping capacities may be significantly lower than previously thought. Therefore, it is of vital importance to gauge this effect and to identify threshold concentrations of organic molecules at which CO₂ storage is significantly affected.

1.3 Objectives of thesis

Given the above motivation and background, the following objectives are set for this thesis:

1. To examine the influence of stearic acid concentration on the wettability of calcite/CO₂/brine systems at ambient conditions and typical storage conditions (pressure 0.1 MPa and 25 MPa respectively, and temperature 323 K), in order to address the uncertainty associated with CO₂ storage in carbonate reservoirs/aquifers.
2. To examine the influence of various organic acids (hexanoic acid, lauric acid, stearic acid, and lignoceric acid) on the wettability of quartz/CO₂/brine systems as a function of acid concentration at ambient and high-pressure conditions (pressure 0.1 MPa, and 25 MPa respectively, at 323 K).
3. To determine the threshold of organic concentrations responsible for wettability reversal, and to improve the understanding of the influence of organics on fluid flow distribution and interfacial phenomenon.

1.4 Organisation of thesis

The thesis has five (5) chapters. Chapter 1 provides an overview of the thesis, including background, motivation, and objectives. Chapter 2 covers a comprehensive literature review, including basic terminology, the physics of the wetting phenomenon at the rock/fluid interface, trapping mechanisms, the existence and origin of organic acids in the porous medium, the chemistry associated with organic acids, previous wettability studies, and the influence of wettability on trapping potential. Chapter 3 describes the methodology of the thesis, which predominantly comprises contact angle measurements and a procedure to age the samples in a given organic acid to mimic the subsurface behaviour. Chapter 4 presents the results, and discusses contact angle measurements of calcite and quartz surfaces as a function of organic acid concentration. Chapter 5 concludes the thesis with future recommendations. Figure 1-1-1 demonstrates a pictorial view of the organisation of this thesis.

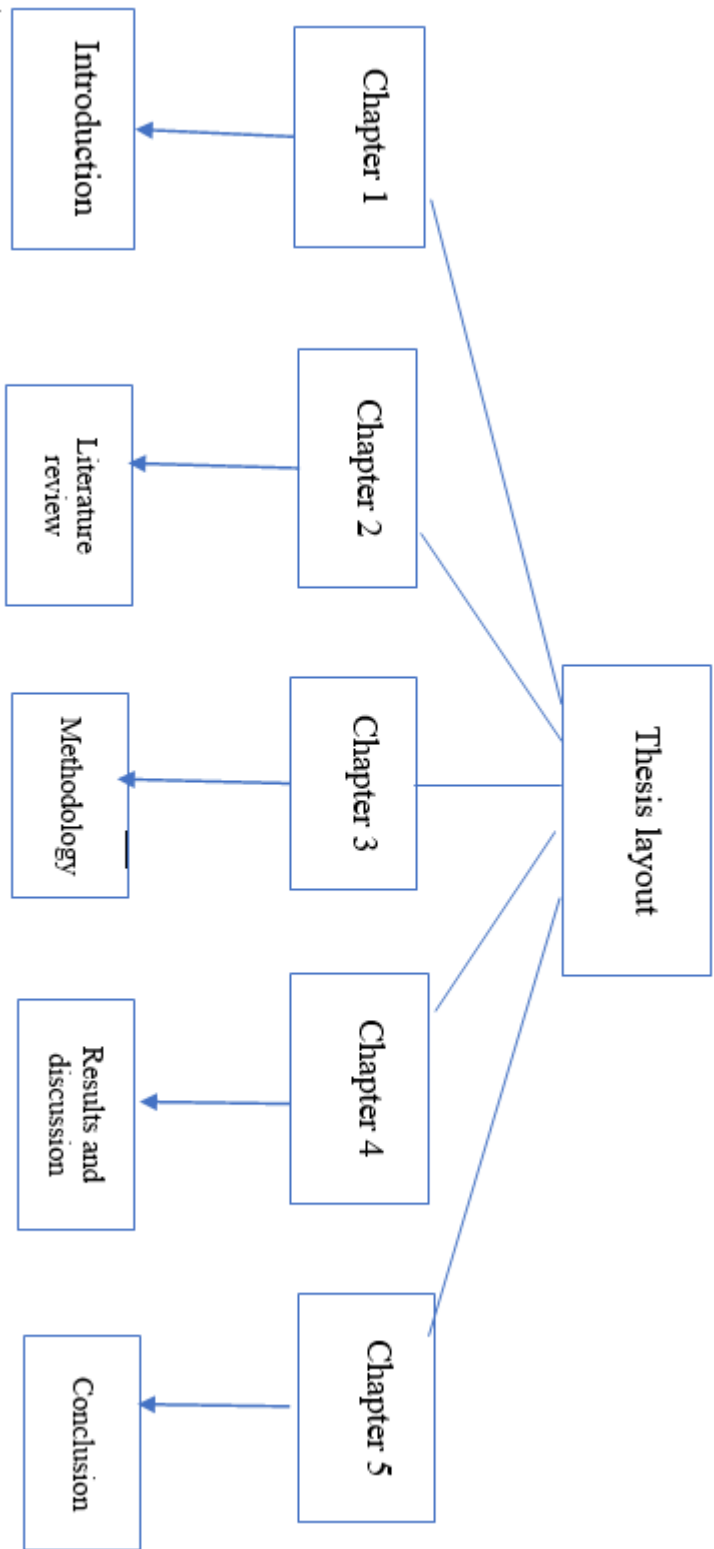


Figure 1-1-1 Thesis layout

Chapter 2 Literature review

2.1 Introduction

This chapter provides a review of the literature in the domain of wettability of rock forming minerals, using a critical analysis from the most fundamental studies to the current knowledge and gaps in the context of geological CO₂ storage. Rock CO₂-wettability plays a vital role in fluid distribution and flow in porous media during CO₂ storage in depleted oil and gas reservoirs or deep saline aquifers. This chapter first describes the phase behaviour of CO₂, with an emphasis on ‘supercritical’ CO₂ behaviour. The focus then shifts to CO₂ storage principles, worldwide statistics of geological storage projects, and potential CO₂ storage options. The trapping mechanisms that are responsible for long-term immobilisation of CO₂ in reservoir rocks are then evaluated. Next, the wettability of rock/fluid systems is defined, and its intrinsic behaviour is depicted by the advancing and receding contact angles. The influence of wettability on structural and residual trapping is also described, forming a basis for the technical evaluation and analysis of the results that are presented in this thesis. The chapter also covers the factors influencing wettability of rock/CO₂/brine systems, with an emphasis on the role of organic acid concentrations in reservoirs; and presents a review of previous studies on the CO₂-wettability of rock forming minerals, such as pure quartz and calcite surfaces.

2.2 CO₂ phase behaviour

Carbon dioxide is a natural and vital constituent of the atmosphere; the concentration typically ranges up to 350 ppm (Rosenberg, 1981). Under all conditions, CO₂ is colourless, odourless, non-flammable, and non-toxic (Haynes, 2014). Figure 2-1 demonstrates the typical phase behaviour diagram of CO₂ at a range of operating pressures and temperatures. Depending on the prevailing pressure and temperature, CO₂ can exist as a gas, liquid, solid, or in a supercritical state (Figure 2-1). Typically, CO₂ maintains a gaseous state below 0.5 MPa and can be liquefied above this pressure. At 0.5 MPa and 56.56 °C, the three possible CO₂ phases can coexist; this is referred to as the triple point (Figure 2-1). The critical point in CO₂ phase behaviour occurs at 7.38 MPa and 31.10 °C. At any pressure and temperature above the critical point, CO₂ exists as a dense liquid phase, more commonly known as a supercritical fluid. Supercritical CO₂ demonstrates properties midway between the gas and liquid phases

(Budisa & Schulze-Makuch, 2014). In oil and gas industry applications of CO₂, including enhanced oil recovery and CO₂ storage, supercritical CO₂ is typically used.

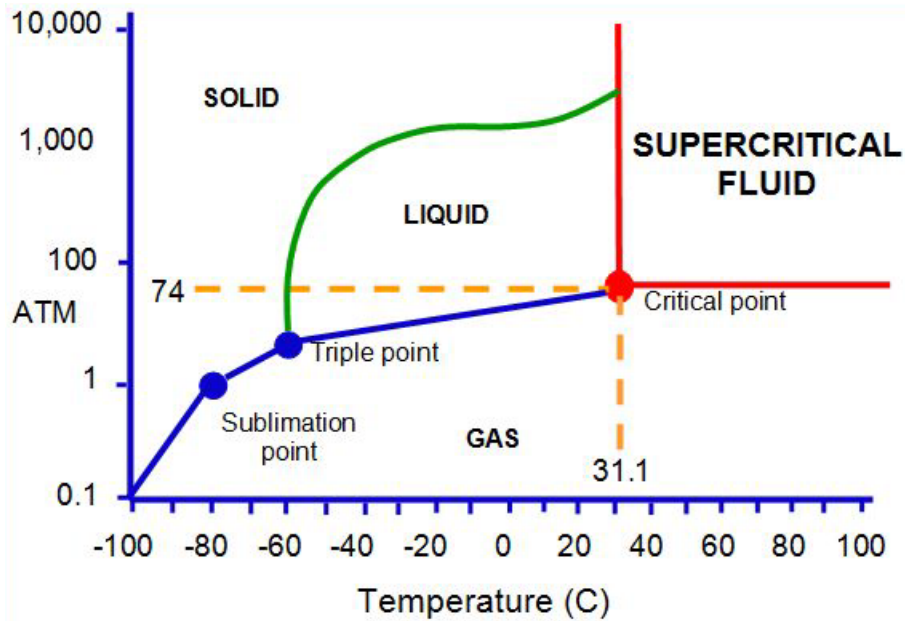


Figure 2-1 CO₂ phase diagram (after King and Bott, 2012).

2.3 Carbon capture and storage

Carbon capture and storage (CCS) refers to a sequence of procedures to capture CO₂ from large point sources and inject it into a geological formation for long-term storage. The purpose is to ensure a cleaner environment by mitigating anthropogenic CO₂ emissions and limiting carbon footprint (Bickle, 2009; Class et al., 2009; IPCC, 2005; Winthaegen et al., 2005).

In principle, the capture and storage of CO₂ consists of three distinct steps, as illustrated in Figure 2-2. The first step is to capture CO₂ from commercial-scale point sources (e.g. coal plants, industries, power generation plants, and chemical treatment plants) or other carbon emitters, and to separate it from impurities in the captured stream. Typically, capture techniques include pre- and post-combustion capture, and oxyfuel combustion (Bhown & Freeman, 2011; Markewitz & Bongartz, 2015). Second, the captured CO₂ is compressed under high pressure (typically 10 MPa) using a compression station (Posch & Haider, 2012). Finally, the compressed CO₂ is transported to a storage site (e.g. an onshore or offshore geological site) by means of pipelines or ships (Pires et al., 2011; Svensson et al., 2004; Zhang et al., 2006).

Because CO₂ is non-flammable, it is much safer to transport than natural gas. Ultimately, CO₂ injection into the underground geological formation commences at a target injection rate and injection pressure; these are based on geochemical and petrophysical assessments using comprehensive screening criteria (Harvey et al., 2012; Kavscek, 2002).

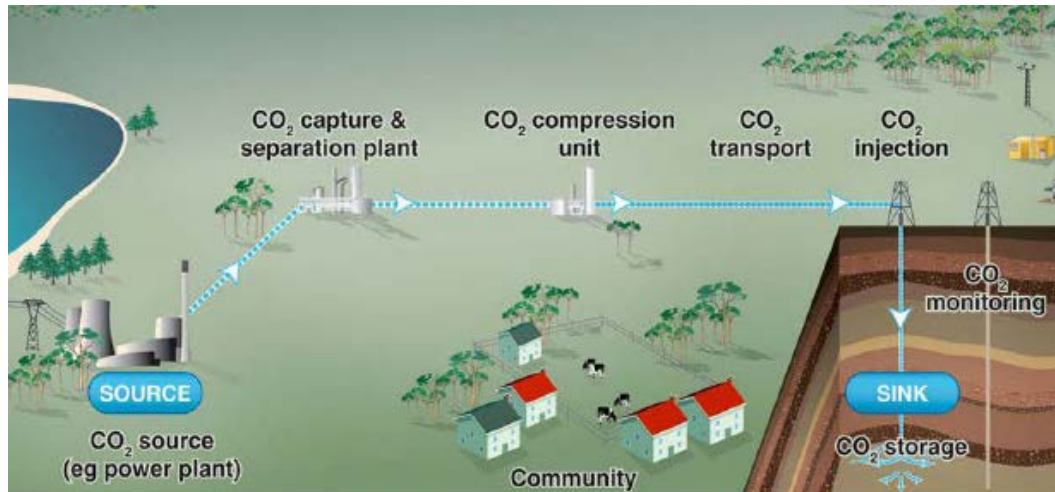


Figure 2-2 A stepwise illustration of the carbon capture and storage procedure (after CO₂CRC web data).

There are several CO₂ sequestration projects in the execution, completion or ongoing stage across the world. Table 2-1 describes the world's largest CO₂ sequestration projects. The Sleipner project in Norway is considered as one of the world's largest sequestration project, aiming to store 1 million tons of CO₂ per year, while the Canadian Weyburn project and the Algerian In Salah project and Australian Gorgon project are other world's largest CO₂ sequestration examples (Thomas and Benson, 2015). Annually, around 3–4 million tons of CO₂ is stored in geological formations (depleted oil and gas reservoirs and deep saline aquifers), demonstrating the significance of underground CO₂ storage.

Table 2-1 Worldwide CO₂ storage projects (modified after IPCC, 2005).

Project	CO ₂ stored (M tons/year)	Storage formation	Project phase
Sleipner (Norway)	1	Saline aquifer sandstone (offshore)	Monitoring and modelling stage
Weyburn (Canada)	1.7	Carbonate reservoir (onshore)	Monitoring, risk assessment, and performance assessment
In Salah (Algeria)	1	Sandstone reservoir (onshore)	Monitoring and risk assessment stage
Gorgon (Australia)	4	Saline aquifer sandstone (onshore)	Not available
Snohvit (Norway)	0.7	Saline aquifer sandstone (offshore)	Not available

2.3.1 Underground storage options

The major benefit of geological storage of CO₂ is that it offers a long-term isolation from the atmosphere via permanent trapping of CO₂ in the reservoir's porous medium. In this context, there are three potential geological sinks suitable for permanent CO₂ storage: 1) active or depleted oil and gas formations (sandstones/carbonates); 2) deep saline aquifer formations; and 3) coal seams (IPCC, 2005; Thomas & Benson, 2015).

Figure 2-3 demonstrates the various options for CO₂ injection and storage. The most commonly used depleted hydrocarbon (oil/gas) reservoirs and deep saline aquifers are carbonate and sandstone formations. Calcite is the dominant mineral in carbonates, whereas sandstones predominantly comprise quartz mineral. Both calcite and quartz are widely used in laboratory studies of CO₂/rock interactions. Carbonate formations are typically more permeable than sandstone, allowing a greater volume of CO₂ to be injected (IPCC, 2005). The caprock, or the 'seal', which provides a safe closure of the reservoir and prevents capillary leakage of CO₂, is typically shale.

Coal seams are also a potential candidate for geological CO₂ storage, offering an opportunity for enhanced methane recovery as well (Arif et al., 2016c; IPCC, 2005). Of all the storage options, saline aquifers are the deepest, while coal seams are located at much shallower depths.

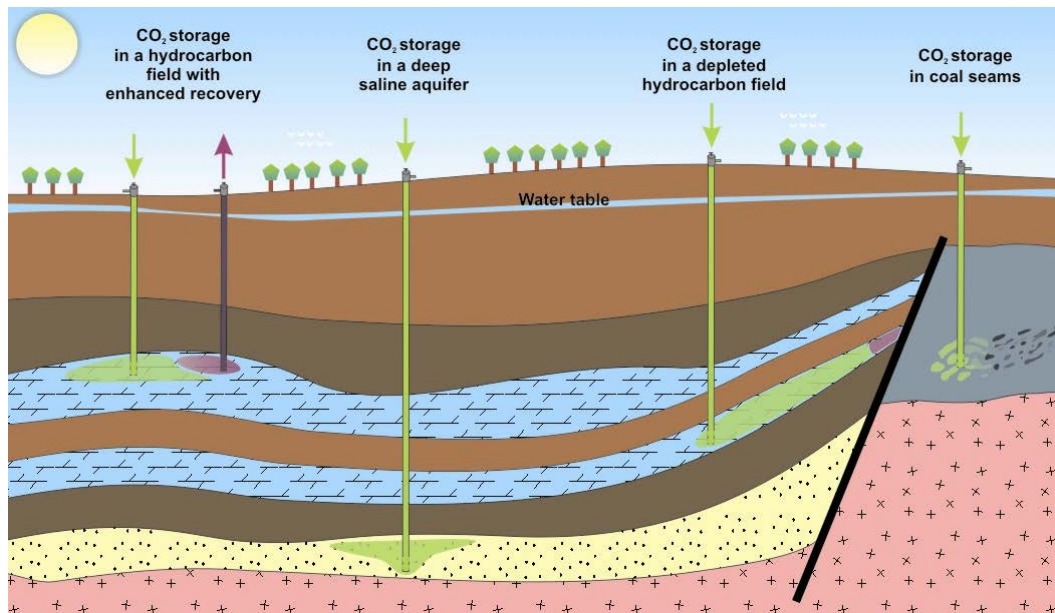


Figure 2-3 Geological CO₂ sequestration options. Extreme left: enhanced oil recovery with CO₂ flooding; centre left: storage in deep saline aquifer; centre right: storage in depleted hydrocarbon reservoirs; extreme right: storage in coal seams (modified after GRREBS web data).

Table 2-2 presents a comparison of the estimated storage capacity and relative advantages and disadvantages of all storage options. Saline aquifers have the highest storage capacity; however, their characterisation is very challenging. Coal seams, on the other hand, offer challenges in terms of CO₂ injection, due to their extremely low permeability (IPCC, 2005).

Table 2-2 Storage capacity estimates and relative merits of storage mediums (after IPCC, 2005).

Storage formation	Storage capacity (Gt CO ₂)	Advantages	Disadvantages
Hydrocarbon reservoirs	675–900	Natural trap by caprock sealing	Storage capacity is limited
Saline aquifers	1,000–10,000	Massive storage volumes due to larger areal extent	Characterisation is challenging
Coal seams	3–200	Located closer to emission sites	Injection is extremely difficult

2.3.2 Trapping mechanisms

Trapping mechanisms are the physical and hydrodynamic methods that prevent upwards migration and leakage of CO₂, and consequently render CO₂ immobile in the porous medium. These trapping mechanisms include structural or stratigraphical trapping, capillary or residual trapping, dissolution trapping, and mineral trapping. Another form of trapping is adsorption trapping, which applies to CO₂ storage in coal seams and organic shales via physical adsorption onto the organic matter (Arif et al. 2017b; Saghafi et al., 2014; ShojaiKaveh et al., 2011, 2012).

2.3.2.1 Structural trapping

After the injection of CO₂ into the reservoir, CO₂ escalates up towards the caprock or seal due to the density difference between the fluids in the reservoir (i.e. CO₂ and brine). This upwards plume migration is also attributed to an imbalance between the capillary forces (which tend to hold the buoyant CO₂ back in the pores of the storage rock) and buoyancy forces (which assist an upwards migration). The migrating plume eventually encounters the caprock or reservoir seal. Caprock is an extremely low permeable rock (typically shale, mudstones, clay or salt domes, with permeability usually measured in nano-darcys), which prevents the flow of the buoyant CO₂ plume (Iglauer et al., 2015a, b). As a result, CO₂ is structurally trapped. Figure 2-4 illustrates the types of structural traps, including a) anticline structural trap, b) normal fault trap, c) stratigraphic fault structural trap, and d) thrust trap structural trap. Structural trapping is typically the major storage mechanism during the first decade of storage (as illustrated in Figure 2-5; Iglauer et al., 2015a).

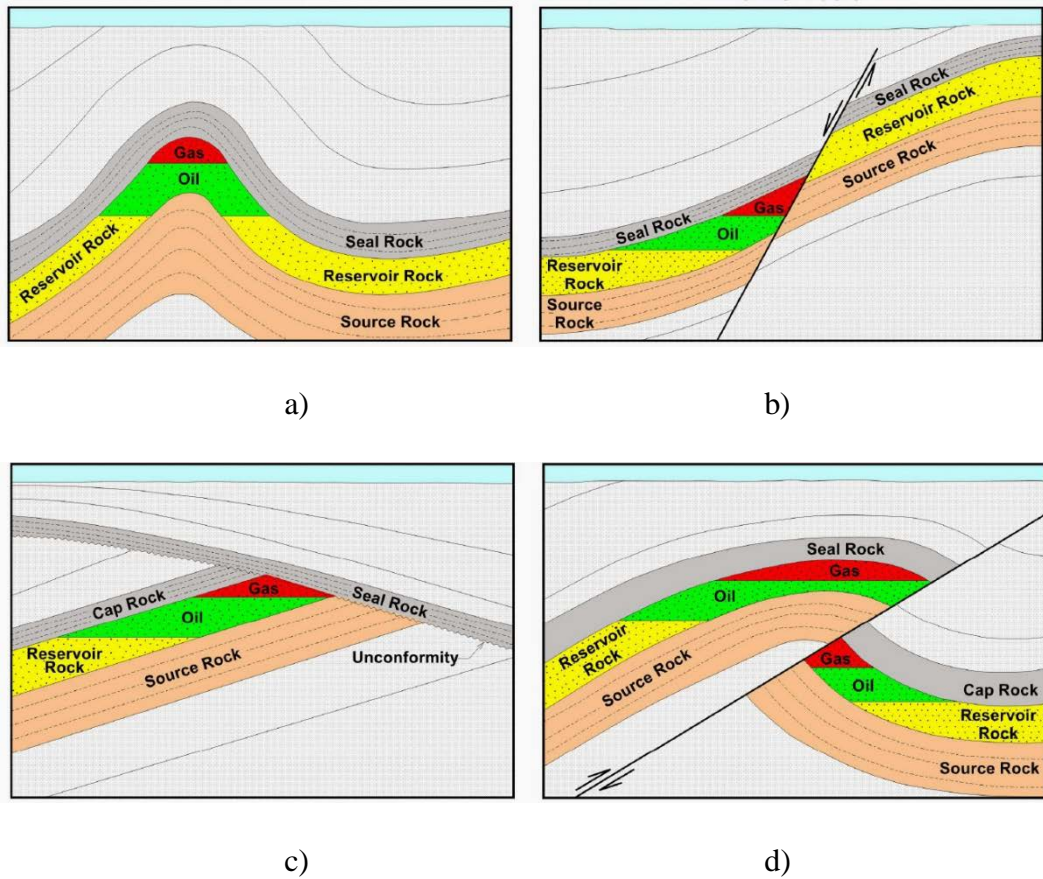


Figure 2-4 Types of structural traps: a) anticline structural trap; b) normal fault trap c) stratigraphic fault structural trap; d) thrust trap structural trap (source: modified after Fundamentals of Petroleum Engineering, module 2, slidershare.net).

2.3.2.2 Capillary or residual trapping

Capillary trapping involves the immobilisation of CO₂ in rock pores due to capillary forces that are of sufficient strength to retain CO₂ (Juanes et al., 2010; Pentland et al., 2011). Capillary trapping takes place when the brine phase displaces CO₂ at the trailing edge of a rising CO₂ plume, resulting in entrapment of CO₂ as discontinuous droplets (see Figure 2-6). Capillary trapping is typically assessed by core flooding displacement experiments on rock-core samples, by measuring the residual CO₂ saturation (Kumar et al., 2005; Qi et al., 2009; Saadatpoor et al., 2010). Capillary trapping is also crucial during the initial decades of the project (Figure 2-5).

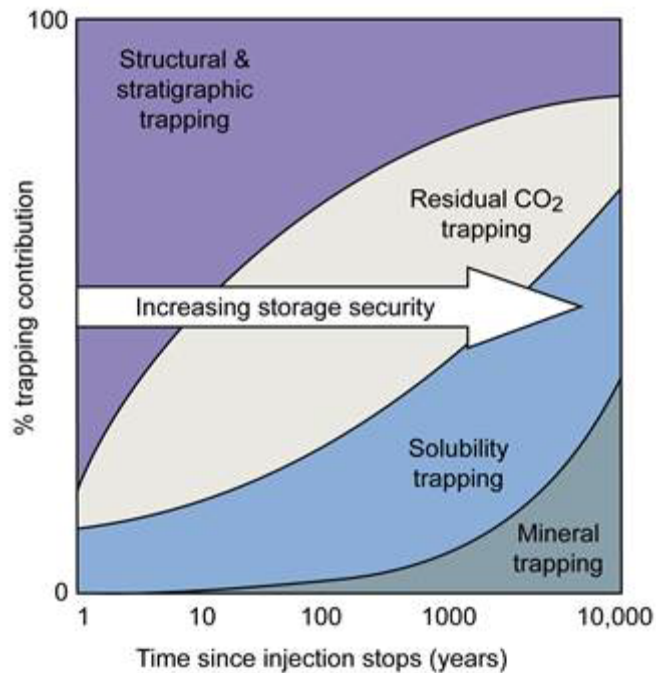


Figure 2-5 CO₂ trapping mechanisms' performance over time (after IPCC, 2005).

2.3.2.3 Solubility trapping

Solubility trapping is a geochemical process by which a dense CO₂-enriched brine is formed by the dissolution of CO₂ in formation brine (Figure 2-6). An important advantage of this mechanism is the absence of a mobile CO₂ plume, due to a small amount of CO₂ dissolved in brine, thereby resulting in improvements in structural and residual trapping capacities (Iglauer, 2011c; IPCC, 2005). Solubility trapping is typically a long-term mechanism, which starts from the middle of a storage project and lasts until the end (Figure 2-5).

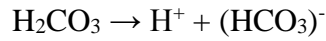
2.3.2.4 Mineral trapping

Mineral trapping involves permanent storage of CO₂ by geochemical reactions between the rock, CO₂ and brine (Pearce et al., 2015), leading to long-term entrapment of massive volumes of CO₂ (Pearce et al., 2015). The stepwise procedure of mineral trapping is illustrated below (Bachu et al., 1994):

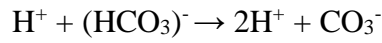
1. Dissolution of CO₂ in brine leading to formation of carbonic acid:



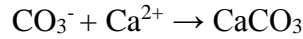
2. Dissociation of carbonic acid leading to formation of bicarbonate ions:



3. Production of more carbonate and hydrogen ions:



4. Precipitation reaction to form calcium carbonate:



Mineral trapping requires a long time to commence; however, once it starts, it can last for hundreds of years (Figure 2-5).

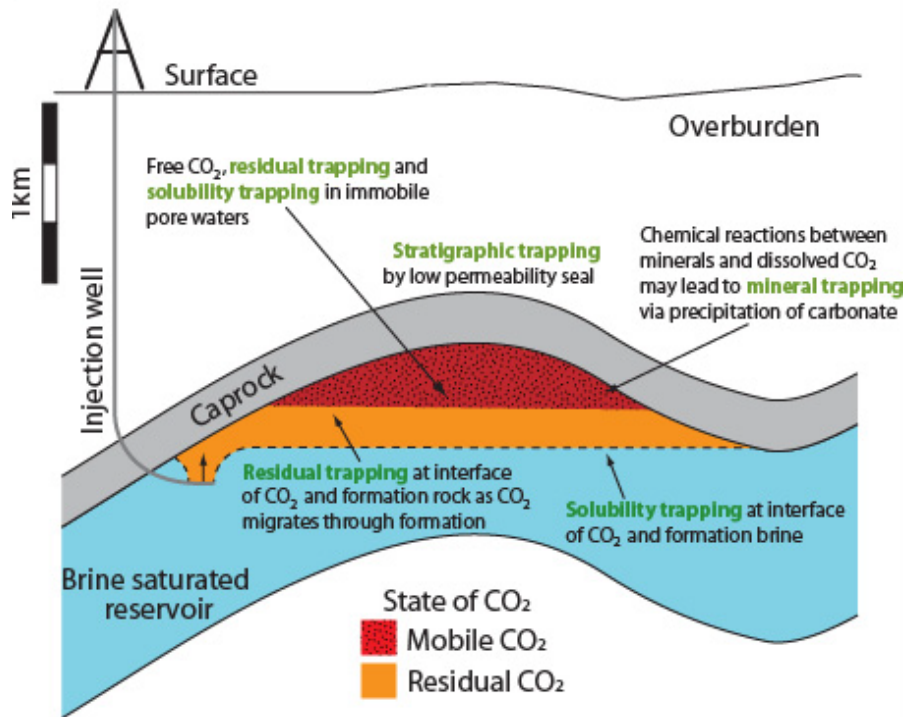


Figure 2-6 Illustration of trapping mechanisms (after Burnside & Naylor, 2011).

2.4 Introduction to rock/fluid wettability

Wettability is the inherent property by which means a solid surface, in the presence of two fluids, tends to remain in contact with one fluid. In the context of hydrocarbon reservoir engineering, wettability is the essential physicochemical parameter that governs fluid distribution and flow dynamics in porous media and residual saturations (Chaudhary et al., 2013; Morrow, 1990, Pentland et al., 2011). Wettability also

influences relative permeability curves and capillary pressure, which are extremely significant for reservoir simulation (Morrow, 1990). Mechanistically, in a rock/oil/water system, if the rock is water-wet, the wetting phase (i.e. water) will occupy the smaller pores, while the non-wetting phase (i.e. oil) will remain in larger pores.

Various experimental approaches are used to measure the wettability of rock/fluid systems including the contact angle measurement, Amott-Harvey index (Amott, 1959), and USBM (Donaldson et al., 1969).

2.4.1 Contact angle method

The contact angle method is widely applied to measure the wetting behaviour of a rock/fluid system. The method typically involves a proxy mineral surface (e.g. calcite for carbonates and quartz for sandstones), whereby a droplet of brine is dispensed onto the surface housed in a cell with CO₂ at a fixed pressure. A reverse configuration also exists, in which a CO₂ bubble is dispensed inside the cell that is filled with brine and contains the mineral surface. The former configuration is referred to as the ‘sessile drop method’, while the latter is known as the ‘captive bubble method’ (Lander et al., 1993). A comparison among various contact angle measurement methods revealed that the sessile drop with tilted plate configuration was the best way to measure wettability of a system (Lander et al., 1993). This technique allows simultaneous measurement of both the receding and advancing contact angles (Lander et al., 1993).

In theory, there are three distinct immiscible phases (solid, water, and air/vapour), which interact with each other and form three different interfaces. This interaction gives rise to three types of interfacial force fields acting on the droplet: solid/water interfacial tension (γ_{sw}), vapour/brine interfacial tension (γ_{vw}), and solid/vapour interfacial tension (γ_{sv}), as shown in Figure 2-7. However, in a mineral/CO₂/brine system, the forces are:

1. mineral/CO₂ interfacial tension (γ_{sc})
2. CO₂/brine interfacial tension (γ_{cw})
3. mineral/brine interfacial tension (γ_{sw}).

Young’s equation demonstrates a force balance of these three interfacial forces and relates them to the macroscopic contact angle, as follows:

$$\cos\theta = \frac{\gamma_{sc} - \gamma_{sw}}{\gamma_{cw}} \quad \text{Eq. 2.1}$$

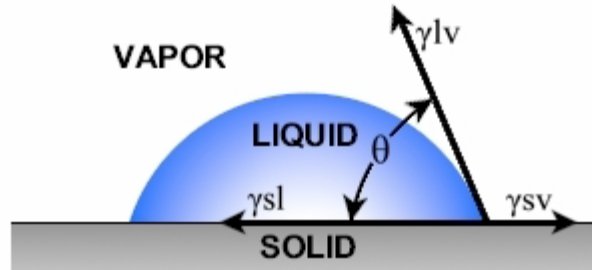


Figure 2-7 Water droplet under interfacial forces in a solid/air/brine system.

Consequently, the contact angle (θ) at the rock/fluid interface governs wettability.

Table 2-3 Wettability regimes for rock/ CO_2 /brine systems on the basis of contact angle (modified after Iglauer et al., 2015a).

Wetting condition	Water contact angle $\theta(^{\circ})$
Complete non-wetting	180
Strongly CO_2 -wet	130–180
Weakly CO_2 -wet	110–130
Intermediate-wet	70–110
Weakly water-wet	50–70
Strongly water-wet	<50
Complete wetting	0

2.4.2 Advancing and receding angles

The tilted plate technique is used to determine the advancing and receding contact angles at both sides of the droplet. At the leading edge of the water droplet (water displacing CO_2), the angle at the rock/ CO_2 /brine interface is the water advancing contact angle (θ_a); this determines the capillary trapping capacity (Chiquet et al., 2007). At the trailing edge of the droplet (CO_2 is displacing brine), the angle is the

water receding contact angle (θ_r); see Figure 2-8. For structural trapping capacity estimation, the water receding contact angle is relevant (Broseta et al., 2012). The difference between advancing and receding contact angles is known as contact angle hysteresis (Broseta et al., 2012).

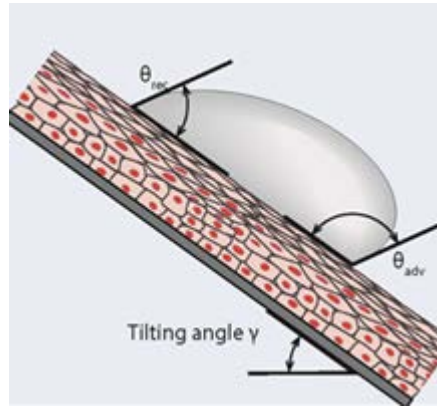


Figure 2-8 Illustration of advancing and receding contacting angles (after Yanez-Soto et al., 2015).

2.4.3 Impact of wettability on structural and residual trapping

To examine the influence of wettability on structural trapping, the equation for the storage height is used, which in turn depicts the capillary sealing efficiency; this is given as:

$$h = \frac{2\gamma_{cw} \cos \theta}{\Delta\rho g R} \quad Eq. 2.2$$

It is clear from Equation 2.2 that structural trapping capacity is a function of CO₂/brine wettability (i.e. contact angle), and interfacial tension. In this context, a strongly water-wet rock (i.e. $\theta < 50^\circ$), leads to a better potential for structural trapping capacities, due in part to increased capillary entry pressure of caprock in water-wet scenarios (Iglauer et al., 2015a). With the decrease in rock's water-wettability, a corresponding reduction in structural trapping potential occurs. For the case of a CO₂-wet caprock, negative values of capillary pressure prevail and thus CO₂ will leak through the caprock (Iglauer et al., 2015a); such situations may lead to a remarkable reduction in structural trapping capacities. In conclusion, water-wet caprocks are often better for storage.

Conversely, capillary trapping is also related to wettability, such that the strongly water-wet system yields much a higher trapped CO₂ saturation; whereas for the strongly CO₂-wet systems, capillary trapping is significantly lower (Chaudhary et al., 2013; Iglauer et al., 2013; Krevor et al., 2015).

2.4.4 Previous studies on CO₂ wettability

2.4.4.1 Pure minerals

In the past few years, CO₂-wettability of minerals has evolved as an emerging research theme, with many studies reporting experimental wettability data for various combinations of mineral/CO₂/brine systems.

Chiquet et al. (2007) reported CO₂-wettability of quartz and mica and found that a mica surface which was strongly water-wet at ambient conditions turned weakly CO₂-wet at high pressure (Chiquet et al., 2007). Broseta et al. (2012) reported CO₂-wettability of calcite and mica at typical storage conditions; both were weakly water-wet, especially at high pressures. Farookhpoor et al. (2013) reported wettability for calcite, mica, and feldspar using experimental measurement of contact angles. Iglauer et al. (2014) conducted a study on the influence of surface-cleaning methods on contact angle, and concluded that surface contamination can lead to highly biased contact angle values. Arif et al. (2016a) conducted a comprehensive study on the CO₂-wettability of mica as a function of pressure and temperature, and concluded that mica surfaces were weakly water-wet at typical storage conditions (15 MPa and 343 K). Saraji et al. (2014) reported experimental wettability data on quartz surfaces, and found that pure quartz surfaces were water-wet even at high pressures. ShojaiKaveh et al. (2016) measured the wettability of shaly caprock and found that caprock CO₂-wettability increased with pressure. They also concluded that structural trapping capacity decreases with an increase in CO₂-wettability. Arif et al. (2017a) evaluated CO₂-wettability of pure calcite, and found that contact angles on calcite surfaces increased with pressure and decreased with temperature (Arif et al., 2017a). In a later study, Arif et al. (2017b) reported CO₂-wettability of organic-rich shales as a function of shale TOC, and found that contact angle increased with TOC in a log-linear relationship. Cahudhary et al. (2015) presented a new method by using high-resolution X-ray computed tomography (HRXCT) and radiography for measuring wettability or contact angle of minerals (muscovite, quartz, borosilicate glass, shale, polyether ether

ketone (PEEK), and polytetrafluoroethylene (PTFE or Teflon) surfaces at different reservoir pressure-temperature conditions and found that PEEK and PTFE surfaces become CO₂-wet at reservoir conditions whereas, quartz and muscovite have showed water-wet characteristics and borosilicate glass have depicted decrease in its water-wetness at reservoir conditions. Gultinan et al. (2017) measured the wettability of CO₂ on organic shale at various organic matter concentrations and thermal maturities and found that bulk organic shale shows strongly water-wet characteristics with respect to CO₂ despite alterations to the thermal maturity and different organic concentrations.

A few other studies have examined the physics of wettability alteration. For example, Arif et al. (2016d) related wettability changes at the brine/mineral interface to the interplay of the three interfacial tensions involved in Young's equation (Equation 2.1). They concluded that solid/CO₂ interfacial tension decreased with pressure, while solid/water interfacial tension increased with temperature; this caused a corresponding wettability shift in coals and mica, whereas the opposite was observed for quartz (Arif et al., 2017d). In addition, studies have used zeta potential measurements to relate wettability to the electrochemical changes at the brine/mineral interface (Alroudhan et al., 2016; Arif et al., 2017c, d; Jackson et al., 2016; Vinogradov & Jackson, 2015).

Iglauer (2017) published a comprehensive review of reported wettability data and the factors influencing wettability of rock/CO₂/brine systems; his published data are reproduced in Figure 2-9. The red and black datapoints are for the minerals/rocks that are hydrophobic, while the green and blue datapoints represent the water-wet or hydrophilic minerals. It can be seen that CO₂ wettability of rock varies from strongly water-wet to strongly CO₂-wet (Iglauer, 2017).

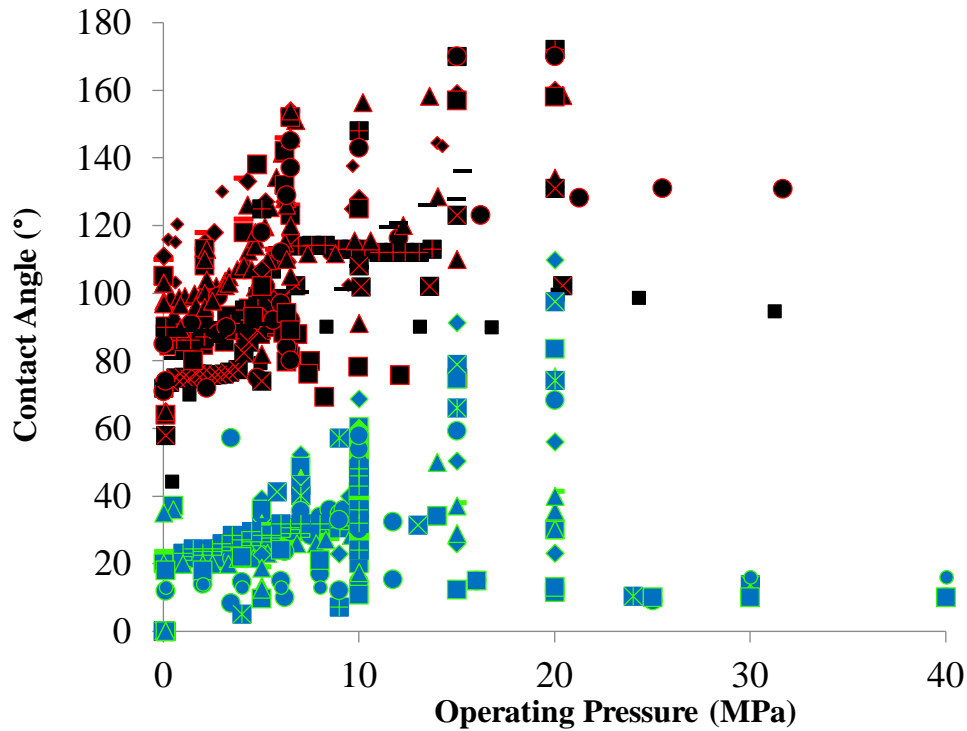


Figure 2-9 Contact angle data for mineral/CO₂/brine systems (modified after Iglauer, 2017).

2.4.4.2 Wettability of altered surfaces

Some studies have reported wettability of surfaces that are aged in silanol (Al-Anssari et al., 2016; Arif et al., 2016b; Dickson et al., 2006) or crude oil (Yang et al., 2007). All such studies found a massive wettability transformation for harsh ageing conditions. For example, Al-Anssari et al. (2016) report that the pure calcite, which is strongly water-wet at ambient conditions, turned into strongly CO₂-wet after ageing in silane solution.

Al-Anssari et al. (2017a, b, c; 2018) reported CO₂-wettability of nano-modified calcite surfaces in a series of publications. The measurements were at high pressure and high temperature conditions, and it was demonstrated that calcite surfaces altered with silica nanoparticles exhibit strongly water-wet characteristics in comparison to pure calcite (Al-Anssari et al., 2018a, b, c; 2018).

2.5 Fatty acids in sediments

During the early 1970s, there was a great deal of geochemical interest in fatty acids, due to the development of new analytical techniques such as gas chromatography to separate the organics from a crude oil stream (Kvenvolden, 1967). Fatty acids are of particular interest to petroleum geochemists, because of evidence that fatty acids are naturally occurring materials in hydrocarbon reservoirs (Waples, 1981). Fatty acids range from straight-chain saturated monocarboxylic acids to branched and straight-chain unsaturated fatty acids (Waples, 1981). Many researches have confirmed the existence of unsaturated straight-chain fatty acid traces in modern sediments and ocean waters (Meredith et al., 2000; Watson et al., 2002). There is experimental evidence of the existence of long-chain monocarboxylic acids in tight sands in Canada (Cyr & Strausz, 1984). Similarly, branched-chain fatty acids are present in hydrocarbons in modern sediments and Green River oil shale (McGowan et al., 1985).

The common acids that are present in reservoirs or aquifers include hexanoic acid, heptanoic acid, stearic acid, lauric acid, and lignoceric or oleic acid (Amaya et al., 2002; Hamouda & Gomari, 2006; Hansen et al., 2000; Kharaka et al., 2009; Jardine et al., 1989; Legens et al., 1998; Madsen and Ida, 1998; Stalker et al., 2013; Yang et al., 2015). The following sections describe previous studies that considered the influence of these organic acids on the wettability of minerals. However, a major limitation is that all of these studies are based on rock/oil/brine wettability, and no study has been undertaken for rock/CO₂/brine systems.

2.6 Influence of organic acids on rock wettability

Our understanding of oil-wet surfaces relates to a series of publications by Andersen (1986). These studies related the oil-wet nature of rock to the adsorption of polar organic compounds present in crude oil (Andersen, 1986). In addition, the acid molecules' diffusion through a water film is another physical mechanism responsible for wettability reversal.

To the best of the author's knowledge, very few studies have reported wettability data as a function of organic acid concentration. These studies are summarised in Table 2-4, and described below.

Table 2-4 Previous wettability studies which considered organic acids.

Reference	System analysed	Organic acids	Operating conditions
Legens et al. (1998)	Calcite/brine/toluene	Benzoic acid, lauric acid	Ambient conditions
Hansen et al. (2000)	Calcite/water/decane	Stearic acid	Up to 30 MPa at 23 °C and 50 °C
Standnes and Austad, (2003)	Calcite/water/heptane	Octanoic acid, lauric acid, stearic acid	Ambient conditions
Gomari et al. (2006)	Calcite/brine/decane	Heptanoic acid, stearic acid	Ambient conditions

Legens et al. (1998) observed the interaction between organic acids (lauric acid and benzoic acid) and calcite powder by contact angle measurements on calcite/toluene/brine systems. The measured values of contact angles were 80° for calcite powder aged in benzoic acid; however, in the presence of lauric acid, the observed contact angle was 150°, a significant increase. The system, which was intermediate-wet in the presence of benzoic acid, turned strongly oil-wet in the presence of lauric acid. Wettability reversal from hydrophilic to a more hydrophobic state implied that the adsorbed molecules directed their polar surfaces towards the minerals (Legens et al., 1998). The conclusion was that the organic acids chemisorbed on the surface calcium ions, that is, they replaced hydroxyl groups on the surface that had resulted from previous hydration by water (Legens et al., 1998). In addition, it was concluded that the calcite surface wettability increased with an increase in the number of carbon atoms of the acid to which it was exposed (Legens et al., 1998).

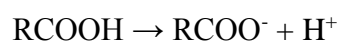
Hansen et al. (2000) conducted an experimental study to observe the adsorption of stearic acid on pure calcite surfaces, to explain the influence of acid concentrations on the wettability of calcite/water/n-decane systems. The advancing and receding contact angles were measured by changing the droplet volume dispensed through the needle. Hansen et al. (2000) used the terms ‘advanced angle’ and ‘receded angle’ to demonstrate the static nature of the observed contact angles. Significantly higher advancing and receding contact angles were measured for calcite + stearic acid/water/n-decane systems. For example, at 30 MPa, advancing angle (θ_a) was as high as 100°, while receding angle (θ_r) was as high as 80° (Hansen et al., 2000).

Standnes and Austad (2003) evaluated the influence of organic acids on the wettability of calcite/oil/brine systems. Contact angles measured were 73° for lauric acid, and 90° for calcite surfaces exposed to stearic acid. This showed that stearic acid, with a larger number of carbon atoms than lauric acid, rendered the calcite surfaces more hydrophobic (Standnes & Austad, 2003). Standnes and Austad (2003) explained this transformation of wettability by organic acids, using a surface complexation model. The wettability alteration due to interaction between organic acids and a calcite surface involves a strong adsorption of carboxylic groups onto the carbonate surface. These molecules play the role of anchors for other polar molecules adsorbing on the rock surface, via dipolar and hydrophobic interaction forces (Standnes & Austad, 2003). Finally, the organic monolayer will cover the entire rock surface (carbonate/calcite), and the rock will turn into oil-wet state. Under such conditions, spontaneous imbibition of water is not possible, due to a negative prevailing capillary pressure caused by the oil-wet nature of rock (Standnes & Austad, 2003).

Gomariet et al. (2006) conducted contact angle measurements on calcite surfaces treated in 0.01 M stearic acid and heptanoic acid. Calcite surfaces that were originally water-wet turned more oil-wet after exposure with stearic acid. The maximum advancing contact angle was 120°, indicating a strongly oil-wet surface (Gomari et al., 2006). Moreover, heptanoic acid turned the calcite surface intermediate-wet at ambient conditions (Gomari et al., 2006).

The literature also identified that directly injecting stearic acid drops through a needle onto the calcite surface can lead to formation of calcium stearate layers, which hinders the process of contact angle measurements (Hansen et al., 2000). Instead, Hansen et al. (2000) used an ageing method by which stearic acid was adsorbed on the freshly cleaved calcite surface placed in 0.02 M stearic acid in n-decane (a supersaturated solution). The samples were aged for 20 h, taken out and rinsed with DI water, and then dried with air before initiating the contact angle measurements (Hansen et al., 2000).

The stearic acid interacts with the calcite surface by means of ionisation of the stearic acid at the calcite/water interface; the following general equation describes the reaction:



This reaction leads to an increase in the pH (the concentration of H^+ ions in the solution), which facilitates the ionisation of the stearic acid. As a result, there is an increase in the tendency of the anionic group $[CH_3(CH_2)_{16}COO^-]$ to dissolve in water. Consequently, once the anionic group interacts with calcite, a chemisorption reaction takes place at the calcite surface, leading to the formation of calcium stearate $[CH_3(CH_2)_{16}COOCa]$. This chemisorption reaction renders the calcite surface more non-wetting (i.e. oil-wet in case of oil/brine/calcite system, and CO_2 -wet in case of CO_2 /brine/calcite system). Using other terms, the calcite surface aged in stearic acid becomes more hydrophobic than the natural untreated calcite surface, which is relatively hydrophilic at ambient conditions.

There is a clear lack of studies into the influence of organic acids on CO_2 -wettability of minerals, despite the proven existence of organic acids in reservoirs as discussed above. Moreover, chemically clean mineral surfaces are artificial, in the sense that they can only be prepared and persist in strongly oxidising environments (Iglauer et al., 2014; Love et al., 2005). In addition, it is well established that anoxic or reducing conditions prevail in the subsurface, i.e. the environment becomes more reducing with increasing depth (Froelich et al., 1979; Townsend et al., 2003). A partial monolayer of small traces of organic acids adsorbed onto the mineral surface is potentially sufficient to cause a total wettability reversal of the system, from strongly water-wet to completely non-wetting (Adamson & Gast, 1997; Hansen et al., 2000; Iglauer et al., 2014). Consequently, consideration of such acids in wettability evaluation is important to reduce the uncertainty associated with wettability predictions.

2.7 Other factors influencing wettability

Various other factors influence wettability, including pressure, temperature, salinity, and surface roughness (Iglauer, 2017). For example, operating pressure significantly affects wettability, and usually an increase in pressure results in an increase in CO_2 /brine/mineral contact angle (i.e. an increase in CO_2 -wettability; Arif et al., 2017a; Al-Anssari et al., 2017a; Iglauer et al., 2015a; Shojai Kaveh et al., 2012). In addition, some studies studied the influence of temperature on the wettability of rock/ CO_2 /brine systems, with some studies reporting a decrease in contact angle with increasing temperature (Arif et al., 2016a, 2017a; Al-Anssari et al., 2017; Bikkina et al., 2011;

Saraji et al., 2013, Shojai Kaveh et al., 2016). Brine composition and salinity also influence the wetting characteristics of rock/CO₂/brine systems. Most studies reported increases in water contact angles with increasing ionic strength of the formation brine (Al-Anssari et al., 2017b; Broseta et al., 2012; Iglauer, 2017; Saraji et al., 2013; Shojai Kaveh et al., 2016). Finally, surface roughness has been found to have a significant influence on wettability. For example, Al-Yaseri et al., (2016) found differences in contact angle values on silica surfaces of different roughness values. Arif et al. (2017a) also reported a decrease in advancing and receding contact angles with increasing surface roughness of calcite.

Chapter 3 Materials and Methods

3.1 Introduction

This chapter details all materials and samples used in this study, and the experimental methods followed. First, the chapter describes the rock samples and fluids used in the study, including their functional properties and other physicochemical features. The rock surface ageing procedure is then outlined, and finally the procedure for contact angle measurements is described.

3.2 Materials

The materials used for the experimental work include fluids, organic acids, mineral samples, and cleaning agent. The following sections describe the specifications of these materials in detail.

3.2.1 Fluids and Salts

Fluids used in this study are listed in Table 3-1.

Table 3-1 Fluids used in this study.

Fluid	Physical state	Resourced from	Purity
Carbon dioxide	Gas, supercritical fluid	BOC Australia, food grade, gas code-082	99.9 mol%
Nitrogen	Gaseous	BOC Australia, food grade, gas code-032	99.9 mol%
Deionised water	Liquid	David Gray	Ultrapure (conductivity = 0.02 mS/cm)
Decane	Liquid	Rowe Scientific	99.9 mol%
Acetone	Liquid	Rowe Scientific	99.9 mol%
NaCl	Solid	Scharlan	99.9 mol%

3.2.2 Organic acids

Organic acids range from short-chain fatty acids to long-chain fatty acids (Haynes, 2014). Fatty acids are a group of carboxylic acids that have a long aliphatic chain that can be either saturated or unsaturated (Speight, 2005). Typically, most of the naturally occurring fatty acids have an unbranched chain of carbon atoms (Speight, 2005).

The naturally occurring fatty acids are classified into four groups: short-chain, medium-chain, long-chain, and very-long chain fatty acids. The associated number of carbon atoms and common examples of each category are shown in Table 3-2.

Table 3-2 Classification of organic acids.

Type of fatty acid	Number of carbon atoms	Examples
Short chain	1–6	Hexanoic acid (C6)
Medium chain	7–12	Lauric acid (C12)
Long chain	13–21	Stearic acid (C18)
Very long chain	22 or more	Lignoceric acid (C24)

As described in Chapter 2, the existence of organic acids in the subsurface has been proven by various studies (Karatha et al., 2009). To analyse the influence of these organic acids on the fluid-rock interfacial interaction, four organic acids were selected, one from each of the types described in Table 3-2: hexanoic acid, lauric acid, stearic acid, and lignoceric acid.

Table 3-3 presents the relevant characteristics of these four organic acids used.

Table 3-3 Organic acids used in this study.

Organic Acid	Physical state	Formula	Number of carbon atoms	Molar mass (g/mol)
Hexanoic acid	Liquid	$C_6H_{12}O_2$	6	116.158
Lauric acid	Powder	$C_{12}H_{24}O_2$	12	200.318
Stearic acid	Powder	$C_{18}H_{36}O_2$	18	284.4772
Lignoceric acid	Powder	$C_{24}H_{48}O_2$	24	368.63

3.2.3 Minerals used

Pure quartz and pure calcite (Iceland spar) from Ward's Natural Science were used in these experiments as representatives of sandstone and carbonate respectively. The calcite sample used had perfect rhombohedral cleavage in three directions not at right angles (120° and 60° ; Hurlbut & Klein, 1985). The quartz and calcite samples used in these experiments were perfectly cleaved by the supplier.

3.2.4 Cleaning agents

In contact angle experimental measurements, the selection of the surface cleaning procedure is vital, because surface contamination can result in very biased contact angle values (Bikkina, 2012; Iglauer et al., 2014; Mahadevan, 2012). Prior to the ageing process, the calcite and quartz samples were cleaned for ~5 minutes by air plasma equipment. After the ageing process, the minerals were cleaned with nitrogen to ensure the organics remained intact.

3.3 Surface roughness

An AFM instrument (DS 95-20DME NanoTechnologie GmbH) was used to determine the surface roughness of all calcite samples used, whereas, surface roughness of quartz samples were provided by supplier. The root-mean-square (RMS) surface roughness of the sample was tested before and after the contact angle measurements. The surface roughness for calcite before the measurement was 4.4 nm and after the measurement was 4.8 nm (detail provided in Chapter 4), whereas, surface roughness of quartz before measurement was 1 to 2 nm (as provided by supplier). These values indicated a smooth surface (when compared with Sarmadivaleh et al., 2015). The surface topographical images are shown in the Appendix.

3.4 Ageing procedure

To simulate a typical storage formation, where the rock pore surfaces are exposed to formation water over geological times (Birkholzer et al., 2009; Ji & Xu, 2015; Nordbotten et al., 2005; White et al., 2003), the following strategy was adopted:

- The calcite samples were immersed for 30 min in calcite-equilibrated DI-water, while the acidity was maintained at pH = 4 by adding drops of aqueous hydrochloric acid, whereas, this process was not done for quartz surfaces because of no effect. This procedure increases the adsorption rate of stearic acid onto the calcite substrate, and thus simulates adsorption over geological times.
- Substrates were cleaned with calcite-equilibrated DI-water for calcite samples and quartz-equilibrated DI-water for quartz samples to remove any dust or surface fragments from the surface.
- N₂ was used to mechanically clean (blow away) the remaining solution on the surfaces to avoid contamination and also removes the thin water film adsorbed from humidity in the air (Stipp et al., 1996).
- The sample was then dried in an oven at 90°C for 60 mins and exposed to air plasma (using a Diemer Yocto instrument) for 15 mins to remove any organic contamination (Love et al., 2005; Iglauer et al., 2014).
- Subsequently, the samples were aged in stearic acid/n-decane solutions of prescribed molarity (10⁻² M to 10⁻¹⁰ M) for seven days to mimic exposure to formation water (which contains organic molecules) over geological times (Gomari & Hamouda, 2006; Hamouda & Gomari, 2006; Karoussi et al., 2008; Tabrizy et al., 2011).
- We consider that the use of decane for wetting alteration is justified for deep saline aquifers, as aquifers are shown to have traces of oil (Bennett et al., 1993) as a result of biodegradation and organic matter diagenesis and subsequent migration into the water zones (Jones et al., 2008).

The ageing procedure adopted in this work is consistent with the literature (Hoeiland et al., 2001; Karoussi et al., 2008).

3.5 Contact angle measurements

Contact angle is considered the best quantitative technique to evaluate the wettability behaviour of a given rock/fluid system under representative conditions (Lander et al., 1993). The benefit of the contact angle measurement method is that it also allows

wettability classification for a wide variety of working situations as a function of operating temperature, pressure, and brine composition (Arif et al., 2017a). In addition, contact angle measurements can be performed for mineral surfaces of different surface roughness (Arif et al., 2017a; Al-Anssari et al., 2018).

Of all available methods for contact angle measurements, tilted plate is regarded as the most effective due to its application to determining both the advancing and receding contact angles simultaneously.

3.5.1 Contact angle measurements setup

This study used the pendant drop tilted plate contact angle method to measure the contact angle (Lander et al., 1993). This setup was used by many previous studies (Arif et al., 2016a, b; Al-Anssari et al., 2017, 2018). Although the decoupling of tangential and lateral forces on the droplet changes with the change in angle of tilt (Eral and Oh, 2013), nevertheless the high reproducibility associated with the tilted plate technique makes it the best method for contact angle measurement. Moreover, this method allows measurement of both the advancing and receding contact angles simultaneously (Lander et al., 1993).

The schematic of the experimental setup is shown in Figure 3-1. It consists of a high-pressure, high-temperature cell, which houses the sample on a tilted plate. It is connected to two pumps, a brine pump and a CO₂ pump. Both pumps are ISCO Teledyne series. The gas cylinder and brine pump are both connected to the parr reactor to allow thermal equilibrium between CO₂ and injected brine before injecting into the measurement cell. Once the fluids have equilibrated, the mixture was injected into the cell at a desired pressure and temperature; the cell temperature is fixed to a desired value for any given measurement. The cell is connected to a temperature bath to maintain the temperature of the system. The system measurements are recorded by a video camera (Basler scA 640–70 fm, pixel size = 7.4 μm; frame rate = 71 fps; Fujinon CCTV lens: HF35HA-1B; 1:1.6/35 mm) which is connected to a computer system to display the results.

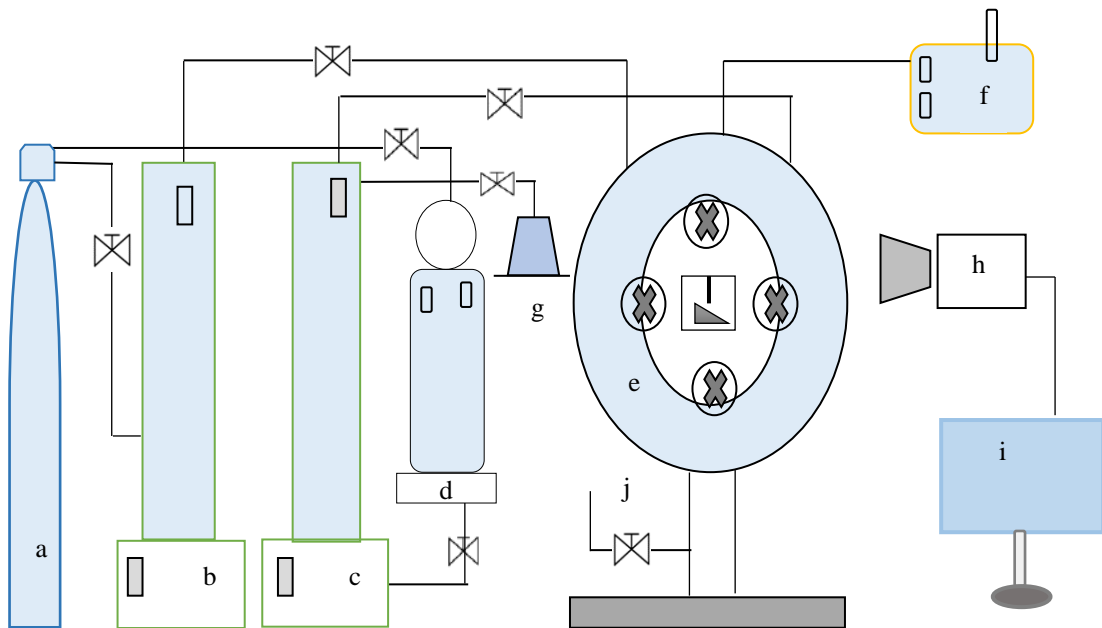


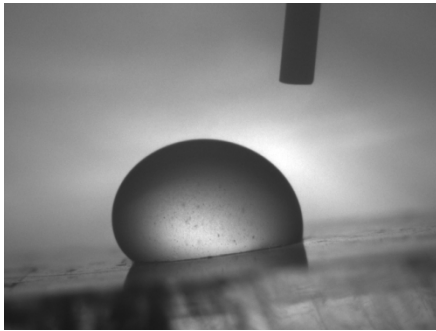
Figure 3-1 Schematic representation of experimental setup used to measure advancing and receding contact angles (modified after Arif et al., 2017a). (a) CO₂ supply; (b) ISCO (high precision syringe pump) for CO₂; (c) ISCO (high precision syringe pump) for brine; (d) high pressure mixing reactor for fluid equilibration; (e) high pressure cell (inside visible with substrate retained on a tilted plate); (f) heating unit and controller for high pressure cell; (g) liquid drain system; (h) high resolution video camera; (i) desktop computer installed with image visualisation and interpretation software; (j) gas pressure relief valve (modified after Arif et al., 2017a).

The following points describe the complete procedure for contact angle measurements:

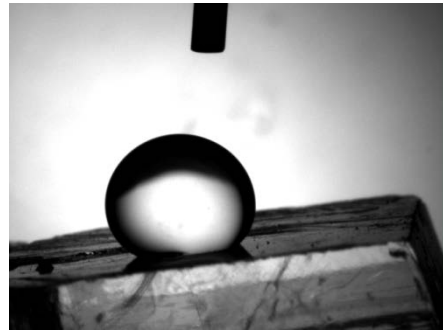
- After aging calcite or quartz sample (of known root mean square surface roughness) was first washed with acetone, dried on 90 °C, and then placed in the cell on the tilted plate (angle of tilt = 17°), and the cell was closed.
- A mixing equilibrating reactor was used to thermodynamically equilibrate the CO₂ and brine (John Morris Scientific, Parr 4848 reactor, mixing frequency = 60 Hz, max. P = 35 MPa, max. T = 350 °C).
- The required temperature (323 K) was customised in the pressure cell. The reactor temperature was also fixed at the same value as cell temperature.

- A high precision syringe pump (ISCO 250D, Teledyne; pressure accuracy of 0.1% FS) was used to inject a constant volume of liquid (~60 ml of de-gassed brine or DI water, vacuumed for 12 hours) in the mixing reactor.
- Subsequently, another high precision syringe pump (ISCO 500D, Teledyne; pressure accuracy of 0.1% FS) was used to pump CO₂ at customised pressure values of 10 MPa and 25 MPa into the reactor.
- After injecting CO₂ and brine into the mixing reactor at the desired temperature and pressure, they were mixed in order to minimise the dissolution and mass transfer effects during contact angle measurements; the equilibration was sustained for ~60 minutes for each measurement.
- The high pressure cell was filled with equilibrated CO₂ at the required experimental pressure and temperature. CO₂ was pumped until it was stabilised on the required pressure and no further injection was required. The pump was set to constant pressure in order to effectively stabilise the system.
- A droplet of equilibrated DI-water/brine (with average volume of 6 μL ± 1 μL), was dispensed through a needle onto the quartz/calcite sample.
- In accordance with DeGennes et al. (2004), the needle size was kept small to reduce the size of the droplet to avoid the effect of droplet size on the contact angle. In these measurements, the minimum capillary length of these droplets is 2.23 mm, which is larger than an average droplet radius on rock surfaces (~1.7 ± 0.2 mm), hence the influence of droplet size on contact angle is negligible.
- Advancing and receding contact angles were measured at the water-CO₂ interface on leading and trailing edges before the movement of the droplet on the rock surface.
- This complete process was recorded and images were extracted from the video to measure the contact angles (Figure 3-2 and Figure 3-3).
- Finally, 'ImageJ' software was used to analyse the images, where the 'angle' icon provided in the menu bar to mark receding and advancing angles on the image.
- The measurements were repeated three times to ensure reproducible values.
- The standard deviation of the measurements was ±3° based on replicated measurements.

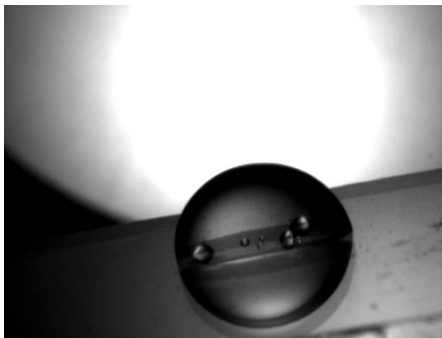
On each new measurement, acetone was used to clean the cell, and DI water was circulated through the pump and flow lines to remove the residual solids and contaminants. The bottom cylinder of the mixing reactor was removed and cleaned with acetone, followed by drying for few hours.



a) 10 MPa, 323 K (calcite/stearic)



b) 25 MPa, 323 K (calcite/stearic)

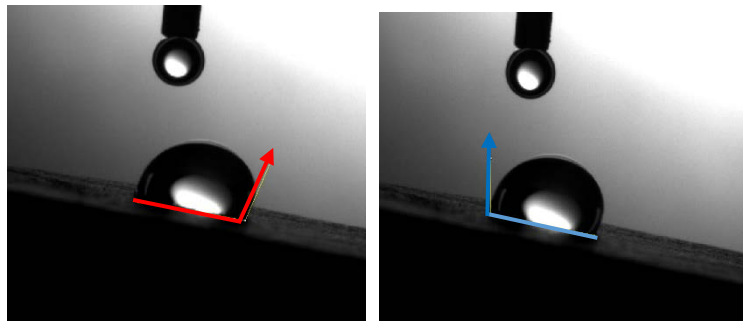


c) 25 MPa, 323 K (quartz/hexanoic)



d) 25 MPa, 323 K (quartz/stearic)

Figure 3-2 Example images extracted from video files for contact angle measurements. Figure (a) and (b) are taken at 10^{-2} M of stearic acid on a calcite surface at 10 MPa and 25 MPa; Figure (c) and (d) are taken at 10^{-2} M of hexanoic acid and stearic acid respectively on a quartz surface at 25 MPa; all were taken at 323 K; CO_2 is in surrounding.



(b)

Figure 3-3 Schematic of contact angle measurements. Right (blue) is ‘receding angle’, and left (red) is ‘advancing angle’ (modified after Arif et al., 2017a).

3.5.2 Imaging procedure

The images were extracted from movie files and visualised in Image analysis software ‘ImageJ’. The analysis was conducted in two different ways:

1) *Manual calculation option:*

In this option, the advancing and receding angles are measured by the observer’s best-fit analysis using an icon called ‘angle’. The tool automatically allows the user to draw both advancing and receding angles on the leading and trailing edge of the water droplet, as shown in Figure 3-3.

2) *Automatic calculation option:*

The software ‘ImageJ’ also includes an automatic contact angle calculation option. Three points are selected at the boundaries of the image: one is the maximum point of the drop shape (the maximum height of droplet), and the other two are at any location. Once points are selected, calculations are automatically done by the software and the values of contact angles are displayed on the screen.

3.6 Summary of operating conditions

The operating conditions in this study were selected to simulate the real subsurface conditions as closely as possible. However, for better scientific understanding, some

measurements were also conducted at ambient conditions. The following sections describe the experimental conditions used in this work.

3.6.1 Calcite

For contact angle measurements on calcite, the measurements were conducted as a function of pressure (10 MPa and 25 MPa) at a constant temperature (323 K). The calcite samples were aged in stearic acid/n-decane solutions of prescribed molarity (10^{-2} M to 10^{-10} M) for seven days to mimic exposure to formation water (which contains organic molecules) over geological time.

3.6.2 Quartz

For quartz, the contact angle measurements were performed as a function of pressure (0.1 MPa and 25 MPa), as a function of temperature (323 K), and as a function of acid type and concentration. The acids used for ageing quartz were hexanoic acid, lauric acid, stearic acid, and lignoceric acid. The concentrations of acids used were 10^{-2} M to 10^{-10} M.

Chapter 4 Results and Discussion

4.1 Introduction

This chapter describes and discusses all the results and analysis in this thesis. The chapter is divided into two key parts. The first part (Section 4.2) describes contact angle results for calcite as a function of pressure and organic acid concentration, and presents and evaluates SEM/EDS and AFM results for calcite.

The second part (Section 4.3) describes the results of contact angle measurements on quartz as a function of pressure, temperature, concentration, and type of organic acid used for ageing the quartz surfaces; the SEM/EDS results for quartz are also analysed, to explain surface-associated morphology and its influence on surface hydrophobicity.

4.2 Calcite Results

For calcite surfaces, the following set of measurements were conducted:

- 1- *Contact angle measurements*: Advancing and receding contact angle measurements were made for calcite/CO₂/brine system, on 9 different calcite surfaces aged in different stearic acid concentrations (10^{-10} M, 10^{-9} M, 10^{-8} M, 10^{-7} M, 10^{-6} M, 10^{-5} M, 10^{-4} M, 10^{-3} M, and 10^{-2} M) at a fixed temperature (323 K). All of these measurements were at two different pressures, 10 MPa and 25 MPa.
- 2- *AFM surface roughness measurements*: the measurements included root mean square (RMS) surface roughness of all the calcite surfaces before and after ageing in stearic acid.
- 3- *SEM/EDS measurements*: The measurements included SEM/EDS images of calcite surfaces before and after contact angle measurements. In addition, measurements of surface composition were also acquired.

The following sections present in detail the results and discussion for calcite.

4.2.1 Surface roughness measurements

RMS surface roughness was measured for the calcite surface before and after ageing in stearic acid. These values are averages over 45 data points measured on five different surface sites for each of the nine samples. Table 4-1 shows the results for average surface roughness for each sample. In summary, the roughness values ranged 4.4 nm to 37.1 nm prior to ageing the surface. After ageing with stearic acid, only a very small increase was found in the surface roughness (Table 4-1). For example, for pure calcite sample 4, the surface roughness before ageing was 37.1 nm, which increased to 37.6 after ageing, an increase in roughness of only 0.5 nm.

Table 4-1 Surface roughness of calcite surfaces before and after ageing in stearic acid

Sample ID	Stearic acid concentration (molarity)	Initial RMS surface roughness (nm), pure calcite	Final RMS surface roughness (nm), treated calcite
1	10^{-2}	4.4	4.84
2	10^{-3}	13.4	13.9
3	10^{-4}	25.3	26.2
4	10^{-5}	37.1	37.6
5	10^{-6}	25.9	26.4
6	10^{-7}	27.2	27.5
7	10^{-8}	18.6	19.2
8	10^{-9}	7.2	7.5
9	10^{-10}	21.6	22.1

Generally, all calcite surfaces used were smooth, which is consistent with Arif et al. (2017a), who reported surface roughness of calcite varying from 7.5 nm to 30 nm. This study does not consider the influence of surface roughness on contact angles. Such an investigation can be found elsewhere (Arif et al., 2017a, Al-Yaseri et al., 2016), where contact angle decreases with increases in surface roughness but that impact is considered when there is huge difference in surface roughness. For example, (Al-Yaseri et al., 2016) have reported that θ_a decreased by 6.5° and θ_r by 2° when surface roughness was increased from (56 nm to 1300 nm). But in this study surface roughness is ranging from 4.4 nm to 37.1 nm which have no significant impact on degree of contact angle variation. Appendix includes the surface topographic images for calcite surfaces.

4.2.2 Contact angle measurements

The results for contact angle measurements on calcite/CO₂/brine system as a function of stearic acid concentration are shown in Figure 4-1 and Table 4-2. The results also include the influence of pressure on contact angle measurements at a constant temperature. The subsequent sections will describe the influence of stearic acid concentration and pressure on contact angles

4.2.2.1 Effect of stearic acid concentration

The calcite surfaces were aged in stearic acid solutions of various concentrations (10⁻² M to 10⁻¹⁰ M). The contact angles on these calcite surfaces were measured at 10 MPa and 25 MPa. Both advancing and receding contact angles for the calcite/CO₂/brine system increased with increasing stearic acid concentration. It can be seen from Figure 4-1 that at 10 MPa and 323 K, for the surface aged in 10⁻¹⁰ M stearic acid, θ_a was 50.2° and θ_r was ~43.1°; this indicates that the surface was strongly water-wet (according to the classification by Iglauer et al., 2015a, as described in Chapter 2). However, with the increase in stearic acid concentration, at a fixed temperature and pressure, both the advancing and receding angles increased consistently. For example, at the same operating temperature and pressure (10 MPa and 323 K), but with the calcite surface aged in 10⁻⁴ M stearic acid, θ_a was 100.9° and θ_r was ~86.5°. This indicates that the surface became intermediate wet (Iglauer et al., 2015a) with the increase in stearic acid concentration in the aquifer or depleted oil reservoir. This also means that structural and residual trapping will be significantly reduced due to the increase in concentration of organic acids in the reservoir, as structural and residual trapping capacities are known to be higher for water-wet reservoirs (Arif et al., 2016a, b; 2017; Iglauer et al., 2015a, b; Krevor et al., 2012). It is also noted that 10⁻¹⁰ M stearic acid is a very low concentration—much higher organics concentrations are measured in deep saline aquifers and certainly in depleted hydrocarbon reservoirs (Kharaka et al., 2009; Stalker et al., 2013; Jardine et al., 1989; Madsen & Ida, 1998; Yang et al., 2015; Thurman, 1985).

Similar trends were observed for all other stearic acid concentrations, i.e. the calcite surface lost its water-wetness (or became more CO₂-wet) with the increase in stearic acid coverage on the surface. The highest values of contact angles were recorded for the calcite surfaces exposed to the highest concentration of stearic acid. For example,

at 10^{-2} M concentration of stearic acid, θ_a was 126° and θ_r was $\sim 98.6^\circ$, indicating that the surface became CO_2 -wet (Iglauer et al., 2015a).

In summary, it is clear from Figure 4-1 and Table 4-2 that even the exposure of minute concentrations of stearic acid to the substrates (which simulates the small amounts of organic molecules in deep saline aquifer and depleted hydrocarbon reservoir storage formations) had a highly significant influence on the water-wetness of the rock. Due to this reduced water-wetness of the surface, the structural trapping capacities can be substantially reduced. Under such high stearic acid concentrations in reservoirs or aquifers, an upwards-directed suction force will lead to an imbalance between capillary and buoyancy forces, resulting in capillary leakage of CO_2 through the caprock (note that capillary leakage is possible at $\theta_r > 90^\circ$; Iglauer et al., 2015b, 2017; Arif et al., 2017b; Naylor et al., 2011).

The optimal capillary trapping limit, which is defined here as the point where primary drainage is unaffected by wettability, is at $\theta_a = 50^\circ$ (Morrow, 1970). Thus, it is evident that capillary trapping can be significantly reduced due to the reduced water-wettability of the surface that was caused by the increase in surface stearic acid coverage.

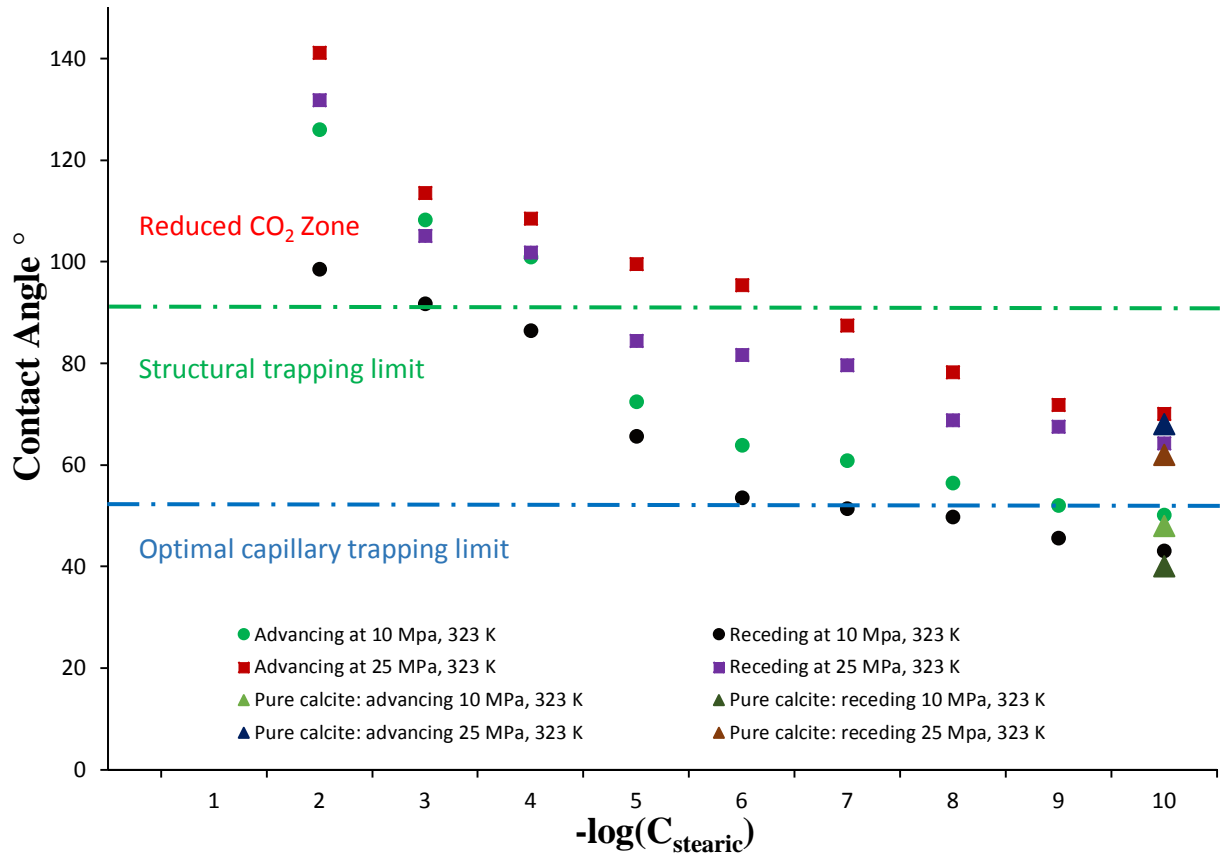


Figure 4-1 Calcite/CO₂/brine contact angles measured as a function of stearic acid concentration at 323 K, and at 10 MPa and 25 MPa; C_{stearic} is the stearic acid concentration (molarity). The green dotted line represents the structural trapping limit, while the blue dotted line represents the optimal capillary trapping limit. The zone above the green dotted line indicates the reduced CO₂ zone.

Table 4-2 Contact angle measurements at different stearic acid concentrations

Stearic acid concentration (molarity)	CO ₂ /calcite/brine contact angle (10 MPa and 323 K)		CO ₂ /calcite/brine contact angle (25 MPa and 323 K)	
	θ_a	θ_r	θ_a	θ_r
10 ⁻²	126.0 ⁿ⁼³	98.6 ⁿ⁼³	141.2 ⁿ⁼³	131.8 ⁿ⁼³
10 ⁻³	108.2 ⁿ⁼³	91.8 ⁿ⁼³	113.5 ⁿ⁼³	105.1 ⁿ⁼³
10 ⁻⁴	100.9 ⁿ⁼³	86.5 ⁿ⁼³	108.5 ⁿ⁼³	101.8 ⁿ⁼³
10 ⁻⁵	72.4 ⁿ⁼³	65.7 ⁿ⁼³	99.6 ⁿ⁼³	84.4 ⁿ⁼³
10 ⁻⁶	63.9 ⁿ⁼³	53.5 ⁿ⁼³	95.4 ⁿ⁼³	81.7 ⁿ⁼³
10 ⁻⁷	60.9 ⁿ⁼³	51.4 ⁿ⁼³	87.5 ⁿ⁼³	79.6 ⁿ⁼³
10 ⁻⁸	56.4 ⁿ⁼³	49.7 ⁿ⁼³	78.2 ⁿ⁼³	68.8 ⁿ⁼³
10 ⁻⁹	52.0 ⁿ⁼³	45.6 ⁿ⁼³	71.8 ⁿ⁼³	67.5 ⁿ⁼³

10 ⁻¹⁰	50.2 ⁿ⁼³	43.1 ⁿ⁼³	70.1 ⁿ⁼³	64.3 ⁿ⁼³
-------------------	---------------------	---------------------	---------------------	---------------------

*n = 3 means that the measurements are repeated three times

4.2.2.2 Effect of pressure on calcite/CO₂/brine contact angles

To analyze the impact of pressure on the aged calcite surfaces, the contact angles were measured at higher pressure (25 MPa). The results are shown in Figure 4-1 and Table 4-2, and are compared with measurements at 10 MPa. The main finding was that both advancing and receding contact angles increased with the increase in pressure. For example, at 25 MPa and 323K, and for calcite surface aged in 10⁻⁵ M stearic acid concentration, θ_a was 99.6° and θ_r was 84.4°, showing that the system was intermediate-wet. However, at the same stearic acid concentration (10⁻⁵ M), but at a lower pressure (10 MPa), lower values of advancing and receding contact angles were recorded such that θ_a was 72.4° and θ_r was 65.7°. This shows that the system that was intermediate-wet at 25 MPa turned into weakly water-wet at 10 MPa. Similar results were found at other concentrations of stearic acid (Figure 4-1, Table 4-2).

The increase in contact angle with pressure can be attributed to the interplay of the three interfacial tensions, as depicted by Young's equation (and explored in detail by Arif et al., 2016d) as follows:

$$\cos\theta = \frac{\gamma_{sc} - \gamma_{sw}}{\gamma_{cw}} \dots\dots\dots \text{Equation (1)}$$

In Equation (1), γ_{sw} , γ_{cw} , and γ_{sc} represent the solid/water, CO₂/water, and solid/CO₂ interfacial tensions respectively. It has been proven that contact angle increases drastically with the increase in pressure; this is due to a reduction in the difference of cohesive energies of the solid and CO₂ with pressure, which leads to more positive interfaces between CO₂ and the solid. As a result, γ_{sc} falls with pressure, which supports de-wetting of the surface (i.e. angles would be higher with high-pressure water contact; Arif et al., 2017).

The increase in contact angle with pressure is consistent with other studies on wettability of pure minerals such as quartz (Saraji et al., 2013; Sarmadivaleh et al., 2015), pure calcite (Arif et al., 2017a), mica (Arif et al., 2016a, b), shales (Arif et al., 2017; ShojaiKaveh et al., 2016), and coal seams (Arif et al., 2016c).

4.2.2.3 Comparison with natural calcite

The contact angles measured on the calcite surfaces aged in stearic acid were also compared with the contact angles on pure unaltered calcite surfaces, as shown by the solid triangle legend in Figure 4-1. It was found that at the same temperature and pressure, the advancing and receding contact angles on aged calcite surface were higher than those for the pure untreated calcite surfaces. For example, Arif et al. (2017a) comprehensively evaluated the wettability of pure calcite surfaces, and reported that, at 10 MPa and 323 K, θ_a was 48° and θ_r was 40° . In contrast, higher values of contact angles were recorded for calcite surfaces aged in even the lowest concentration of stearic acid. For example, for the surface aged in 10^{-10} M stearic acid, θ_a was 50.2° and θ_r was $\sim 43.1^\circ$. The increase in contact angle for the aged calcite surface is attributed to surface coverage by stearic acid (or stearate).

Mechanistically, the stearic acid esterifies the hydroxyl groups on the calcite surface in a condensation reaction (Figure 4-2; Heberling et al., 2011; Mihajlović et al., 2013; Shi et al., 2010). Consequently, the octadecanoate groups (C18 ester groups) chemically (covalently) bond to the calcite surface, rendering them strongly hydrophobic (Al-Anssari et al., 2016).

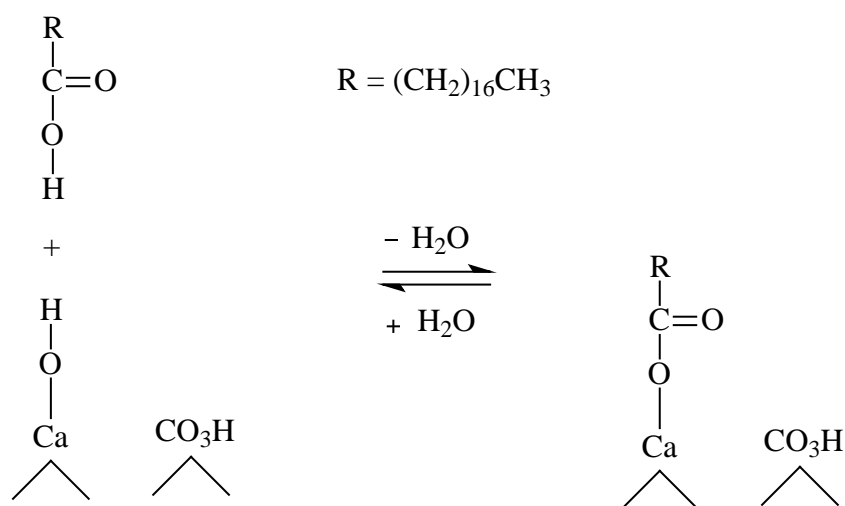


Figure 4-2 (Reaction Scheme) Chemisorption of stearic acid ($\text{CH}_3(\text{CH}_2)_{16}\text{-COOH}$) on solid calcite surface (\wedge indicates solid bulk) (sources: Cao et al., 2016; Heberling et al., 2011; Mihajlović et al., 2013; Shi et al., 2010; Wang et al., 2006).

Moreover, excess carbon coverage of the surface also influences wettability and typically renders the aged calcite surfaces more hydrophobic. This hydrophobicity occurs due to a corresponding deficiency of the surface silanol groups, which is consistent with Dickson et al. (2006) who conducted a similar study on quartz surfaces that were aged in crude oil. Dickson et al. (2006) reported that the contact angle was higher for the surface with higher organic coverage, and that the more hydrophobic surfaces had fewer silanol functional sites, which caused them to be more non-wetting.

4.2.2.4 SEM/EDS analysis of calcite surfaces

Table 4-3 represents the surface composition before and after ageing in stearic acid for all samples tested. Pure calcite mainly comprises calcium (Ca), carbon (C), and oxygen (O). Calcium percentage in the samples ranged from 18.6 wt% to 28.3 wt%, carbon ranged from 18.4 wt% to 24.9 wt%, oxygen percentage was up to 59.8 wt%. After ageing, however, the carbon percentage clearly increased while oxygen and calcium demonstrated a corresponding decrease. Thus, upon exposure to stearic acid, the calcite surface tended to show a deficiency in calcium and oxygen sites on surface with an increase in carbon coverage of the surface; this was consistent with Dickson et al. (2006). Appendix 1 includes some of the selected SEM micrographs of calcite surfaces for both the pure and altered calcite surfaces.

Table 4-3 SEM/EDS composition analysis of calcite surfaces

Sample ID	Stearic Acid (molarity)	Pure calcite			After ageing		
		wt% Ca	wt% C	wt% O	wt% Ca	wt% C	wt% O
1	10^{-2}	24.9	18.8	56.3	23.2	22.3	54.5
2	10^{-3}	25.8	18.4	55.9	23.2	21.5	55.3
3	10^{-4}	25.1	21.3	53.6	24.8	24.5	50.7
4	10^{-5}	22.0	20.0	58.0	21.6	22.9	55.5
5	10^{-6}	28.0	24.9	47.2	22.1	27.9	50.0
6	10^{-7}	24.0	20.4	55.7	22.5	22.0	55.5
7	10^{-8}	25.6	20.0	54.4	20.9	21.4	57.8
8	10^{-9}	28.3	19.6	52.1	28.2	20.8	51.0
9	10^{-10}	18.6	21.5	59.8	18.0	22.6	59.4
Pure calcite	0	20.9	20.1	59.0	20.9	20.1	59.0

4.3 Quartz Results

The following describes the experiments conducted for the quartz surface:

- 1- *Contact angle measurements*: Advancing and receding contact angle measurements were made for quartz/CO₂/brine system for a wide range of organic acid concentrations (10⁻¹⁰ M, 10⁻⁹ M, 10⁻⁸ M, 10⁻⁷ M, 10⁻⁶ M, 10⁻⁵ M, 10⁻⁴ M, 10⁻³ M, and 10⁻² M) for four organic acids (hexanoic, lauric, stearic and lignoceric). Contact angle measurements were conducted at a fixed temperature (323 K), and at different pressures i.e. ambient (0.1 MPa) and 25 MPa.
- 2- *AFM surface roughness measurements*: Surface roughness was provided by supplier ranging up to 2 nm. Appendix 2 includes the surface topographic images for quartz surfaces.
- 3- *SEM/EDS measurements*: The measurements included SEM/EDS images of the quartz surface before and after contact angle measurements. In addition, surface composition measurements have also been acquired.

4.3.1 Contact angle measurements

The following sections describe the results for the contact angle measurements:

4.3.1.1 AFM measurements

AFM measurements were provided by supplier. Overall, all the quartz surfaces were ultra-smooth, with RMS surface roughness ranging up to only 2 nm.

4.3.1.2 Influence of organic acids on quartz wettability

The results of contact angle measurements are provided for quartz surfaces aged in hexanoic acid (Figure 4-3, Table 4-4 and Table 4-5), lauric acid (Figure 4-4, Table 4-4 and Table 4-5), stearic acid (Figure 4-5, Table 4-4 and Table 4-5), and lignoceric acid (Figure 4-6, Table 4-4 and Table 4-5). Both advancing and receding contact angles increased with the increase in concentration of the acids throughout the tested experimental matrix.

Table 4-4 Contact angle measurements at different concentrations of different organic acids at (0.1 MPa and 323 K)

Organic concentration (Molarity)	Hexanoic Acid CO ₂ /Calcite/brine contact angle (0.1 MPa and 323 K)		Lauric Acid CO ₂ /Calcite/brine contact angle (0.1 MPa and 323 K)		Stearic Acid CO ₂ /Calcite/brine contact angle (0.1 MPa and 323 K)		Lignoceric Acid CO ₂ /Calcite/brine contact angle (0.1 MPa and 323 K)	
	θ_a	θ_r	θ_a	θ_a	θ_r	θ_r	θ_a	θ_r
10 ⁻²	59.19	47.79	66.14	59.04	68.62	59.76	75.12	70.28
10 ⁻³	55.15	45.1	62.3	53.41	66.02	57.37	70.83	68.27
10 ⁻⁴	53.5	42.49	61.39	51.01	62.15	53.12	66.89	64.9
10 ⁻⁵	48.44	40.95	58.72	49.82	56.57	49.56	63.55	56.87
10 ⁻⁶	45.1	38.52	53.41	44.08	52.03	47.57	59.02	54.66
10 ⁻⁷	44.8	38.1	48.18	40.32	51.91	42.4	57.2	51.02
10 ⁻⁸	38.23	31.52	44.3	37.4	51.84	42.3	55.98	47.69
10 ⁻⁹	37.84	30.89	43.7	36.9	51.47	41.9	55.36	45.32
10 ⁻¹⁰	37.12	30.42	42.26	36.27	51.19	41.78	54.4	43.11

Table 4-5 Contact angle measurements at different concentrations of different organic acids at (25 MPa and 323 K)

Organic concentration (Molarity)	Hexanoic Acid CO ₂ /Calcite/brine contact angle (25 MPa and 323 K)		Lauric Acid CO ₂ /Calcite/brine contact angle (25 MPa and 323 K)		Stearic Acid CO ₂ /Calcite/brine contact angle (25 MPa and 323 K)		Lignoceric Acid CO ₂ /Calcite/brine contact angle (25 MPa and 323 K)	
	θ_a	θ_r	θ_a	θ_a	θ_r	θ_r	θ_a	θ_r
10 ⁻²	86.97	81.27	89.2	83.81	94.69	84.8	110.41	105.17
10 ⁻³	82.44	75.39	85.92	80.34	87.19	81.72	107.64	96.92
10 ⁻⁴	73.7	70.84	82.52	77.58	83.01	78.83	94.88	86.63
10 ⁻⁵	66.23	61.31	78.52	72.37	79.02	74.05	85.14	78.89
10 ⁻⁶	59.54	57.44	70.76	64.18	76.7	71.8	80.95	73.77
10 ⁻⁷	59.1	57.21	65.23	59.39	70.75	67.35	78.29	71.81
10 ⁻⁸	58.7	56.97	62.72	57.16	65.41	62.56	75.42	67.62
10 ⁻⁹	58.5	56.72	61.12	56.89	65.28	62.32	72.15	65.62
10 ⁻¹⁰	58.2	56.44	60.92	56.34	64.98	61.56	68.86	64.69

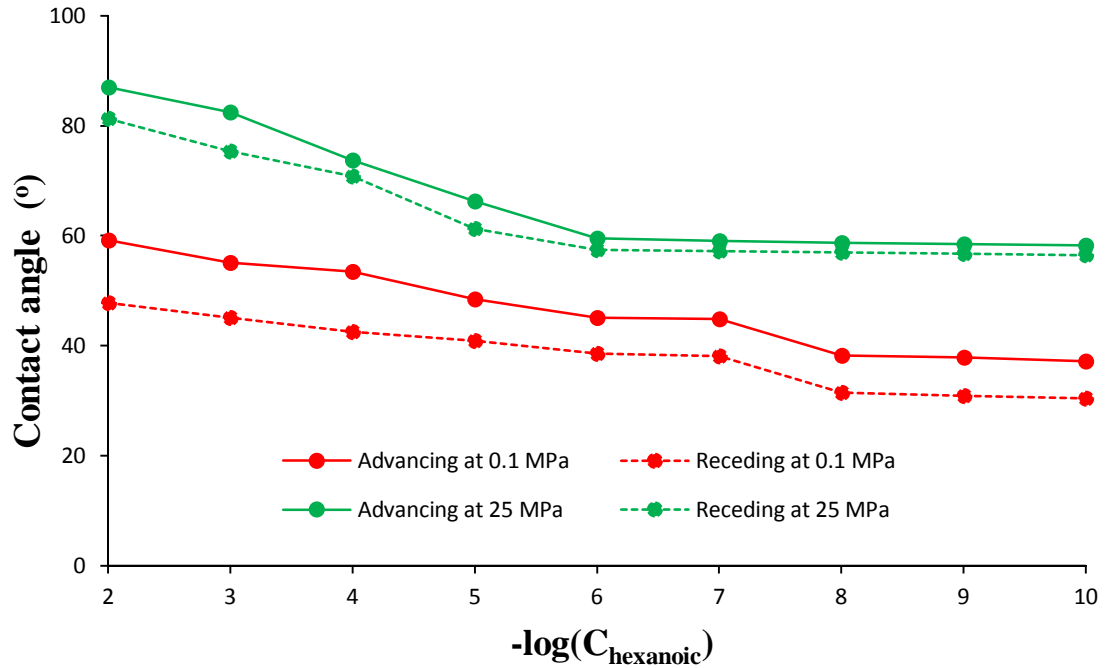


Figure 4-3 Quartz/CO₂/brine contact angles as a function of hexanoic acid concentration; C_{hexanoic} is the hexanoic acid concentration (molarity). Solid lines: advancing; dotted lines: receding. Red: ambient pressure; green: 25 MPa.

For example, at 25 MPa and 323 K, for the quartz surface aged in 10^{-10} M hexanoic acid, θ_a was 58.2° and θ_r was 56.44° , showing that the quartz surface is weakly water-wet under such conditions. With the increase in concentration of hexanoic acid up to 10^{-6} M, there was an insignificant change in contact angles. However, further increases in concentration did result in significant changes in contact angles. For example, when the hexanoic acid concentration increased to the relatively high value of 10^{-2} M, at the same temperature and pressure (25 MPa and 323 K), θ_a and θ_r increased to 86.97° and 81.27° respectively, which is a significant increase (Figure 4-3). This also shows a wettability transformation from weakly water-wet to intermediate-wet. Such a reduction in water wettability of the surface leads to a reduction in structural and residual trapping capacities (Al-Manhali et al., 2016; Chaudhary et al., 2013; Iglauer et al., 2015a, b; Rahman et al., 2016).

Lauric acid followed similar trends. For the quartz surface aged in 10^{-10} M lauric acid, quartz/CO₂/water contact angles were significantly lower than for the surfaces aged in 10^{-2} M lauric acid; higher organic concentration rendered the surface more non-

wetting. For example, at 25 MPa and 323 K, for the quartz surface aged in 10^{-10} M lauric acid, θ_a was 60.92° and θ_r was 56.34° ; these increased to $\theta_a = 89.2^\circ$ and $\theta_r = 83.81^\circ$ when lauric acid concentration increased to 10^{-2} M (Figure 4-4).

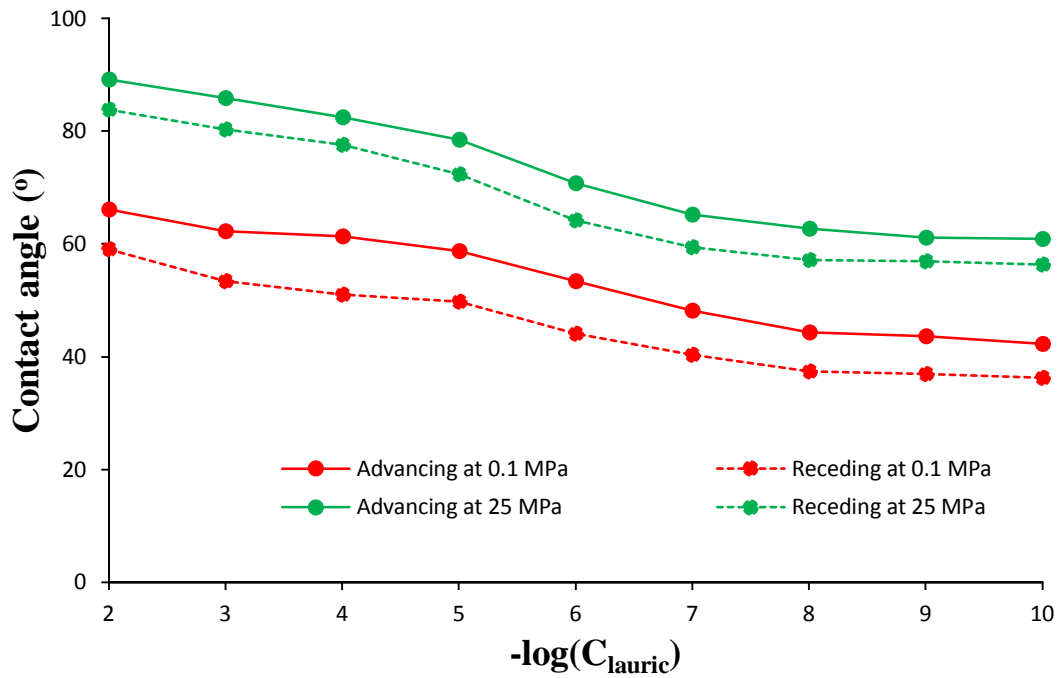


Figure 4-4 Quartz/ CO_2 /brine contact angles as a function of lauric acid concentration; C_{lauric} is the lauric acid concentration (molarity). Solid lines: advancing; dotted lines: receding. Red: ambient pressure; green: 25 MPa.

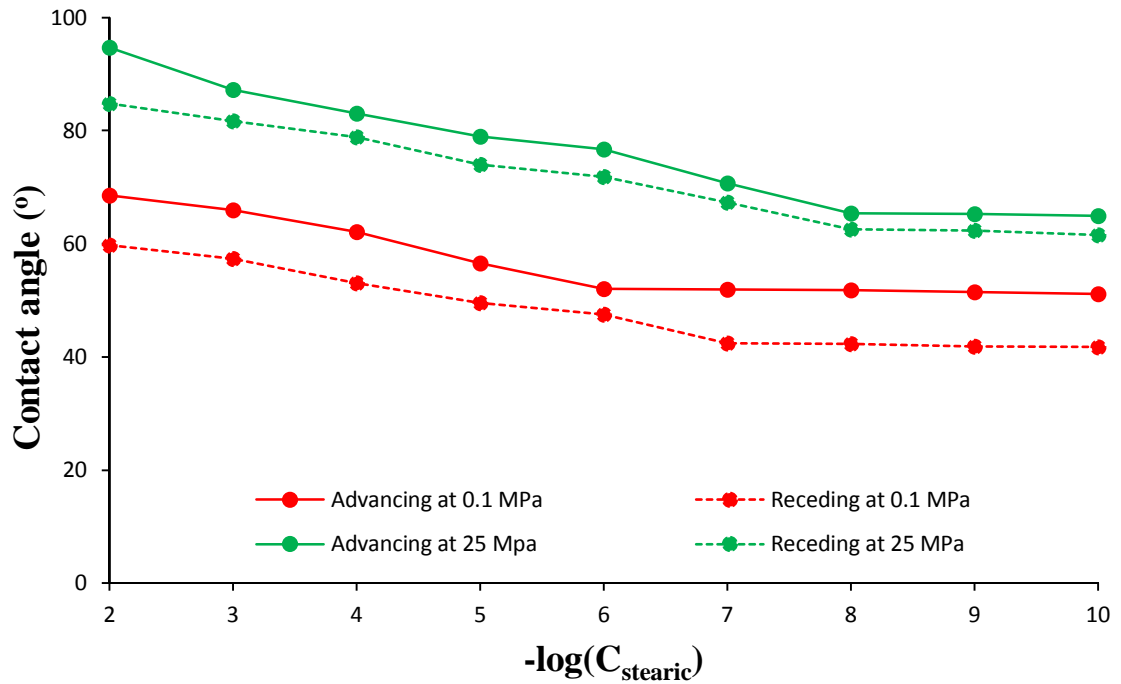


Figure 4-5 Quartz/CO₂/brine contact angles as a function of stearic acid concentration; C_{stearic} is the stearic acid concentration (molarity). Solid lines: advancing; dotted lines: receding. Red: ambient pressure; green: 25 MPa.

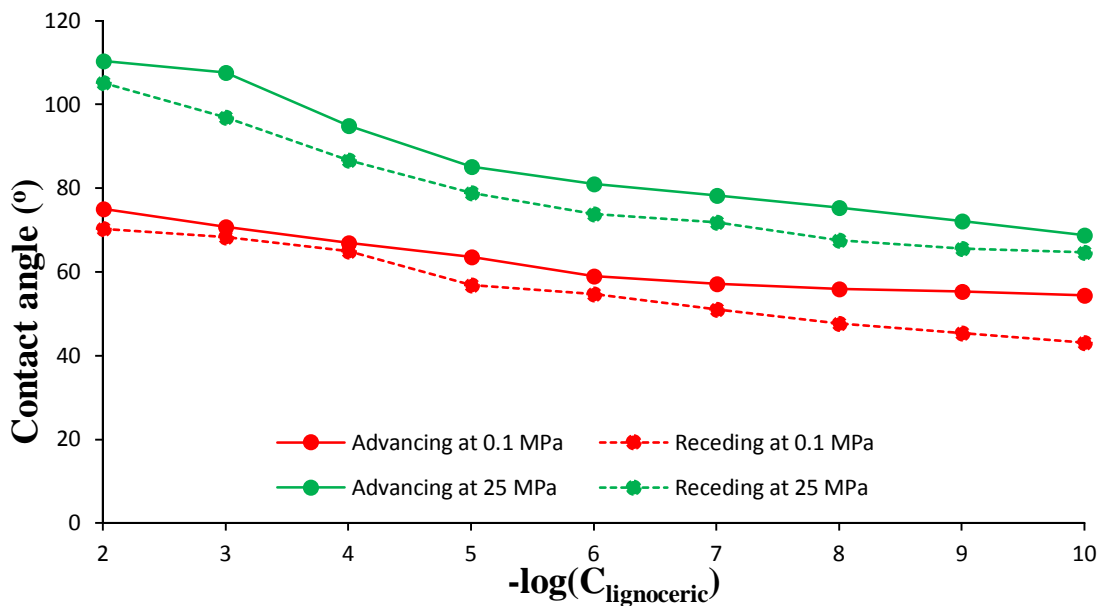


Figure 4-6 Quartz/CO₂/brine contact angles as a function of lignoceric acid concentration; $C_{\text{lignoceric}}$ is the lignoceric acid concentration (molarity). Solid lines: advancing; dotted lines: receding. Red: ambient pressure; green: 25 MPa.

Similar results were found for quartz surfaces aged in stearic acid and lignoceric acid (Figure 4-5 and Figure 4-6). In summary, the higher the organic acid concentration, the higher the values of both the advancing and receding contact angles, irrespective of the type of acid used for ageing.

4.3.1.3 Influence of type of organic acid on quartz

To demonstrate the influence of the type of organic acid on quartz wettability, a plot of advancing and receding contact angles as a function of organic acid concentration for all four acids (hexanoic acid, lauric acid, stearic acid, and lignoceric acid) is shown in Figure 4-7.

It is clear that the organic acids influence the quartz wettability in a similar manner, i.e. both advancing and receding angles increase with increasing concentration of organic acid. However, at a fixed concentration of organic acid, the absolute values of contact angles are different for different acids. Surfaces aged in hexanoic acid exhibit the lowest values of contact angles, while surfaces aged in lignoceric acid exhibit the highest values of contact angles; lauric acid and stearic acid were intermediate. For example, at 25 MPa and 323 K, and a fixed organic concentration (10^{-5} M) of hexanoic acid (θ_a was 66.23° and θ_r was 61.31° ; see red solid and dotted lines in Figure 4-7), showing that the aquifer or reservoir under such conditions is weakly water-wet. However, if the same reservoir had 10^{-5} M of lauric acid, the system would lose its water-wetness ($\theta_a = 78.52^\circ$ and $\theta_r = 72.37^\circ$; see green solid and dotted lines in Figure 4-7). Moreover, if the same reservoir/aquifer contained 10^{-5} M stearic acid, the system would turn intermediate-wet ($\theta_a = 79.02^\circ$ and $\theta_r = 74.05^\circ$; see black solid and dotted lines in Figure 4-7); and with 10^{-5} M lignoceric acid, the water wettability of the system would reduce further ($\theta_a = 85.14^\circ$ and $\theta_r = 78.89^\circ$; blue solid and dotted lines in Figure 4-7).

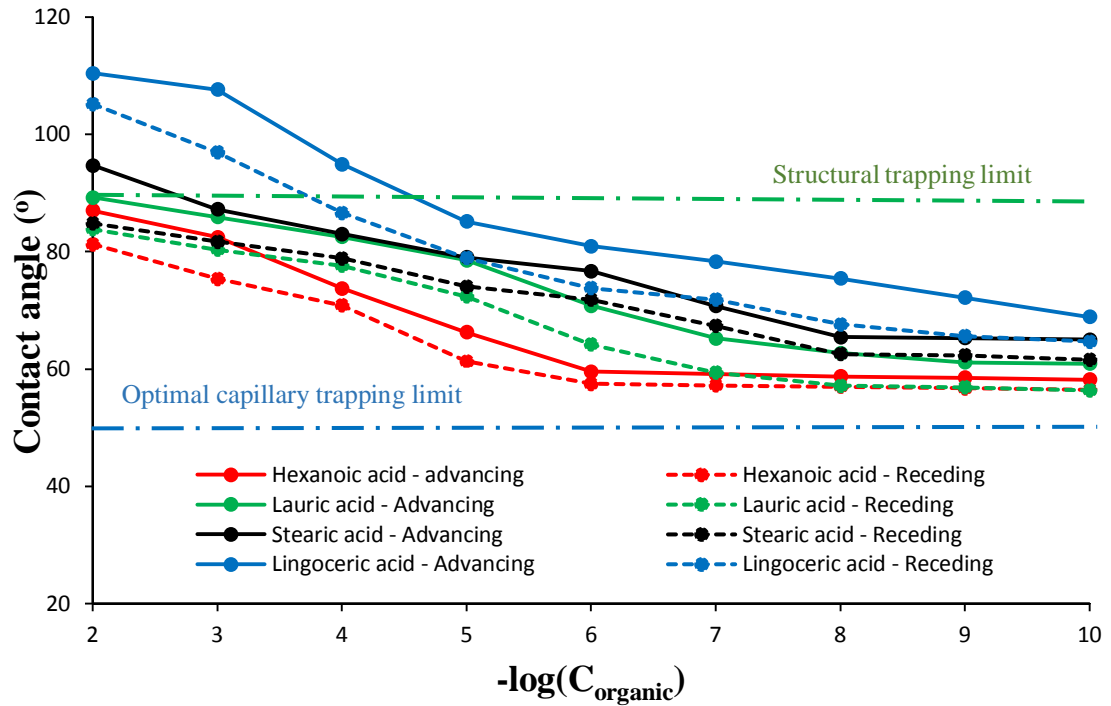


Figure 4-7 Quartz/CO₂/brine contact angles as a function of different organic acid concentration at 25 MPa and 323 K; C_{organic} is the different organic acid concentration (molarity). Dotted blue horizontal lines in the graph define the threshold of capillary trapping ($\theta = 50^\circ$), and Dotted green horizontal lines in graph define the threshold for structural trapping ($\theta > 90^\circ$).

In addition, at the highest tested concentration (10^{-2} M), advancing angle on the quartz surface aged in hexanoic acid, lauric acid, stearic acid, and lignoceric acid were 86.97° , 89.2° , 94.69° and 110.41° respectively, while the receding angles were 81.27° , 83.81° , 84.8° , and 105.17° respectively (Figure 4-7). Thus, a reservoir/aquifer that is intermediate-wet in the presence of a particular concentration of hexanoic acid turns into weakly CO₂-wet in the presence of lignoceric acid (Figure 4-7). Under such CO₂-wet conditions, an upward-directed suction force is created, which results in an imbalance between the capillary and buoyancy forces leading to capillary leakage; this promotes capillary leakage of CO₂ through the caprock (Arif et al., 2017a, b; Iglauer et al., 2017; Krevor et al., 2012). Such a transformation of wettability from water-wet to CO₂-wet by shifting the acid type from hexanoic acid to lignoceric acid is attributed to the number of carbon atoms present in the acid. Lignoceric acid (C₂₄H₄₈O₂) has 24 carbon atoms, whereas hexanoic acid (C₆H₁₂O₂) has 6 carbon atoms. As a result,

higher carbon presence in lignoceric acid renders the surface more hydrophobic. In summary, CO₂-wettability of quartz aged in various organic acids increases with an increasing number of carbon atoms in the organic acid prevailing in the reservoir/aquifer.

4.3.1.4 SEM of quartz

SEM images were obtained for quartz aged in each of the four acids used. SEM mineralogy results are presented for quartz surfaces aged in hexanoic acid (Table 4-6), lauric acid (Table 4-7), stearic acid (Table 4-8), and lignoceric acid (Table 4-9). Selected images are shown in the Appendix.

All SEM tables demonstrate similar trends. The most significant finding is that, after ageing, a considerable increase in percentage of carbon is recorded, which demonstrates adsorption of acid on the quartz surface.

Table 4-6 SEM/EDS of quartz surfaces aged in hexanoic acid

Hexanoic acid concentration (molarity)	Pure quartz			After ageing			Change due to ageing		
	wt% Si	wt% C	wt% O	wt% Si	wt% C	wt% O	wt% Si	wt% C	wt% O
10 ⁻²	31.9	2.3	65.8	38.1	4.8	57.1	+6.2	+2.5	-8.7
10 ⁻³	33.3	4.1	62.6	30.3	7.5	62.2	-3.0	+3.4	-0.4
10 ⁻⁴	35.4	2.8	61.8	37.0	4.9	58.1	+1.6	+2.1	-3.7
10 ⁻⁵	34.7	3.2	62.1	34.2	5.1	60.7	-0.5	+1.9	-1.4
10 ⁻⁶	29.0	3.5	67.5	32.9	5.2	61.9	+3.9	+1.7	-5.6
10 ⁻⁷	29.5	4.2	66.3	29.0	5.8	65.2	-0.5	+1.6	-1.1
10 ⁻⁸	32.8	1.8	65.4	48.0	2.3	49.7	+15.2	+0.5	-15.7
10 ⁻⁹	29.9	3.4	66.7	33.1	4.1	62.8	+3.2	+0.7	-3.9
10 ⁻¹⁰	31.8	2.6	65.6	32.0	2.9	65.1	+0.2	+0.3	-0.5
0	34.0	1.5	64.5	34.0	1.5	64.5	0	0	0

Table 4-7 SEM/EDS of quartz surfaces aged in lauric acid

Lauric acid concentration (molarity)	Pure quartz			After ageing			Change due to ageing		
	wt% Si	wt% C	wt% O	wt% Si	wt% C	wt% O	wt% Si	wt% C	wt% O
10 ⁻²	38.1	2.4	59.5	27.6	5.3	67.1	-10.5	+2.9	+7.6
10 ⁻³	33.8	1.8	64.4	31.1	3.5	65.4	-2.7	+1.7	+1.0
10 ⁻⁴	33.0	3.4	63.6	28.8	6.1	65.1	-4.2	+2.7	+1.5

10 ⁻⁵	38.3	4.3	57.4	35.4	7.1	57.5	-2.9	+2.8	+0.1
10 ⁻⁶	32.4	2.6	65.0	34.1	4.0	61.9	+1.7	+1.4	-3.1
10 ⁻⁷	34.5	3.6	61.9	33.5	5.2	61.3	-1.0	+1.6	-0.6
10 ⁻⁸	32.4	4.1	63.5	32.7	5.4	61.9	+0.3	+1.3	-1.6
10 ⁻⁹	32.4	1.4	66.2	36.1	1.7	62.2	+3.7	+0.3	-4.0
10 ⁻¹⁰	32.2	3.5	64.3	32.8	4.1	63.1	+0.6	+0.6	-1.2
0	31.6	2.3	66.1	31.6	2.3	66.1	0	0	0

Table 4-8 SEM/EDS of quartz surfaces aged in stearic acid

Stearic acid concentration (molarity)	Pure quartz			After ageing			Change due to ageing		
	wt% Si	wt% C	wt% O	wt% Si	wt% C	wt% O	wt% Si	wt% C	wt% O
10 ⁻²	35.4	1.3	63.3	32.2	3.1	64.7	-3.2	+1.8	+1.4
10 ⁻³	34.3	3.7	62.0	26.8	7.6	65.6	-7.5	+3.9	+3.6
10 ⁻⁴	37.0	4.5	58.5	26.7	8.4	64.9	-10.3	+3.9	+6.4
10 ⁻⁵	36.8	1.6	61.6	32.3	2.8	64.9	-4.5	+1.2	+3.3
10 ⁻⁶	35.8	2.4	61.8	41.7	3.8	54.5	+5.9	+1.4	-7.3
10 ⁻⁷	36.0	4.3	59.7	22.0	6.3	71.7	-14.0	+2.0	+12
10 ⁻⁸	38.2	2.9	58.9	23.8	4.0	72.2	-14.4	+1.1	+13.3
10 ⁻⁹	34.1	4.2	61.7	23.5	5.2	71.3	-10.6	+1.0	+9.6
10 ⁻¹⁰	36.5	4.1	59.4	45.4	4.9	49.7	+8.9	+0.8	-9.7
0	36.5	2.2	61.3	36.5	2.2	61.3	0	0	0

Table 4-9 SEM/EDS of quartz surfaces aged in lignoceric acid

Lignoceric acid concentration (molarity)	Pure quartz			After ageing			Change due to ageing		
	wt% Si	wt% C	wt% O	wt% Si	wt% C	wt% O	wt% Si	wt% C	wt% O
10 ⁻²	37.3	2.3	60.4	25.0	6.2	68.8	-12.3	+3.9	+8.4
10 ⁻³	36.3	2.0	61.7	25.4	4.6	70.0	-10.9	+2.6	+8.3
10 ⁻⁴	34.1	4.0	61.9	21.9	7.8	70.3	-12.2	+3.8	+8.4
10 ⁻⁵	35.6	3.4	61.0	24.8	6.2	69.0	-10.8	+2.8	+8.0
10 ⁻⁶	34.7	3.5	61.8	32.3	5.8	61.9	-2.4	+2.3	+0.1
10 ⁻⁷	33.9	4.1	62.0	28.9	6.1	65.0	-5.0	+2.0	+3.0
10 ⁻⁸	33.7	2.7	63.6	26.0	3.9	70.1	-7.7	+1.2	+6.5
10 ⁻⁹	39.6	1.9	58.5	27.7	2.5	69.8	-11.9	+0.6	+11.3
10 ⁻¹⁰	36.5	4.2	59.3	25.0	5.1	69.9	-11.5	+0.9	+10.6
0	34.0	3.6	62.4	34.0	3.6	62.4	0	0	0

4.3.1.5 Comparison of quartz and calcite

It was found in section 4.2 that calcite CO₂-wettability significantly changed in the presence of stearic acid. To understand the relative impact of stearic acid concentration

on quartz and calcite, contact angle data for both surfaces at 25 MPa and 323 K is plotted in Figure 4-8. At any given concentration of stearic acid, both advancing and receding contact angles were higher for calcite and lower for quartz. This is consistent with the intrinsic wettability behavior of pure quartz and calcite. Natural quartz is strongly water-wet under ambient conditions and under typical storage conditions (Saraji et al., 2013; 2014; Sarmadivaleh et al., 2015); however, wettability of pure calcite varies between weakly water-wet to weakly CO₂-wet at pressures up to 20 MPa (Arif et al., 2017a; Broseta et al., 2012; Yang et al., 2007). Upon ageing the surfaces in organic acids, the relative impact of acid on the calcite surface is higher, while aged quartz still remains relatively more water-wet compared to aged calcite (Figure 4-8).

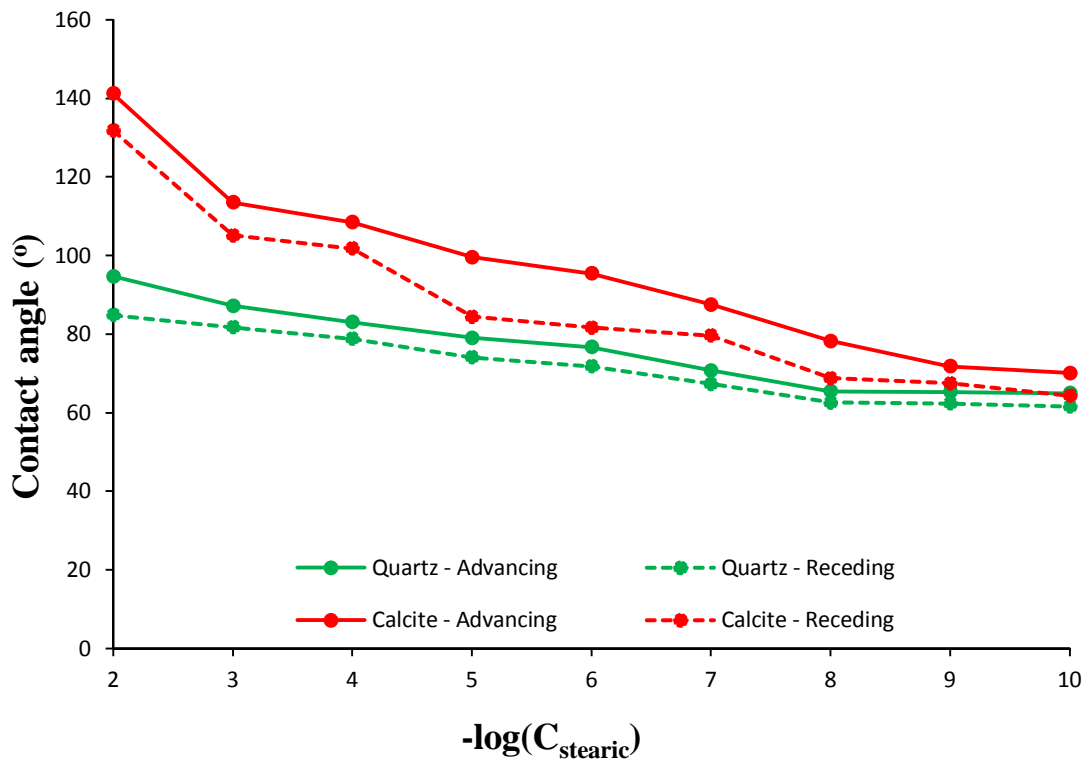


Figure 4-8 Quartz vs. calcite wettability (aged in stearic acid at 25 MPa and 323 K) C_{stearic} is the stearic acid concentration (molarity).

Mechanistically, the following general reaction depicts the adsorption of organic acids on quartz surfaces (Figure 4-9):

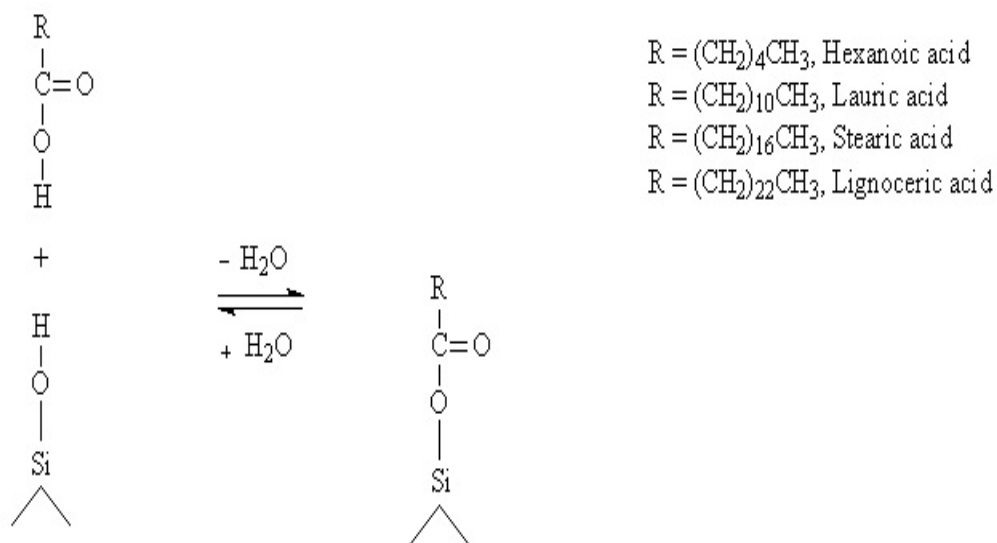


Figure 4-9 (Reaction Scheme) Chemisorption of different organic acids on solid quartz surface (\wedge indicates solid bulk).

4.3.1.6 Influence of pressure

Figure 4-3 to Figure 4-6 show the contact angle measurements for various acids at ambient pressure (0.1 MPa) and high pressure (25 MPa) at a constant temperature (323 K). At ambient conditions, the contact angles on quartz surfaces aged in any of the organic acids are much lower than that at 25 MPa. This is consistent with the wettability of natural quartz at ambient conditions (Sarmadivaleh et al., 2015). At high pressure, significantly higher values of contact angles were recorded.

Chapter 5 Conclusions and Recommendations

5.1 Conclusion

This work reported wettability measurements on calcite/CO₂/brine and quartz/CO₂/brine systems as a function of organic acid type and concentration at typical storage conditions, in order to mimic a more realistic subsurface behaviour. Deep saline aquifers and depleted hydrocarbon reservoirs have organic acids present, which have a direct influence on the interfacial phenomenon at the fluid/rock interface caused by chemisorption of short-chain and long-chain acids. Consequently, there is a direct impact of such organic concentrations on CO₂ geological storage capacity. Moreover, it is clear that a precise knowledge of the influence of acid concentration during CO₂ storage is essential to ensuring safe and long-term geological storage.

The key findings of this work are summarised below:

- Pure calcite, which is typically weakly water-wet under storage conditions, turned weakly CO₂-wet to strongly CO₂-wet after exposure to stearic acid.
- CO₂-wettability of calcite increased with the increase in concentration of stearic acid.
- Increase in operating pressure compounded the effect of stearic acid on calcite wettability, as both advancing and receding contact angles demonstrated a clear increase with pressure.
- Structural trapping limit ($\theta_r > 90^\circ$) and optimal capillary trapping limit ($\theta_a = 50^\circ$) are clearly defined and their thresholds are clearly showed in graphs (Figure 4-1 and Figure 4-7) with respect to each concentration of organic acid in calcite and quartz surfaces.
- Quartz showed similar trends as calcite. With increasing concentration of all organic acids tested, the quartz surface gradually lost its water-wetness.
- For quartz surfaces, at 25 MPa and 323 K, and at the highest tested organic acid concentration (10^{-2} M), the highest values of contact angles were recorded for lignoceric acid, and the lowest values were recorded for hexanoic acid. This is attributed to the number of carbon atoms in the acid. Therefore, this study concludes that the higher the number of carbon atoms in organic acid, the higher the resulting CO₂-wettability of the system.

- A comparison of calcite and quartz surfaces both aged in stearic acid at the same concentrations revealed that the relative impact of organic acids is greater on the calcite surface than quartz.

5.2 Recommendations

This study recommends that the following limitations be addressed for further insights into the influence of organic acids on rock surface wettability:

- The current data apply to carbonate/limestone and sandstone formations with a range of arbitrary concentrations of organic acids. A field scale analysis of the actual composition of organic acids may provide better insights.
- The data assumes pure calcite and quartz, while in real scenarios caprock composition may be different; consequently, the applicability of the reported measurements will be limited.
- Simulation models should account for the influence of organic acids on rock/fluid interactions.

References

- Adamson, A. W., & Gast, A. P. (1997). The solid–liquid interface-contact angle. *Physical Chemistry of Surfaces*, 4, 333-361.
- Agartan, E., Trevisan, L., Cihan, A., Birkholzer, J., Zhou, Q., & Illangasekare, T. H. (2015). Experimental study on effects of geologic heterogeneity in enhancing dissolution trapping of supercritical CO₂. *Water Resources Research*, 51(3), 1635-1648.
- Al-Anssari, S., Barifcani, A., Wang, S., & Iglauer, S. (2016). Wettability alteration of oil-wet carbonate by silica nanofluid. *Journal of Colloid and Interface Science*, 461, 435-442.
- Al-Anssari, S., Arif, M., Wang, S., Barifcani, A., Lebedev, M., & Iglauer, S. (2017a). CO₂ geo-storage capacity enhancement via nanofluid priming. *International Journal of Greenhouse Gas Control*, 63, 20-25.
- Al-Anssari, S., Arif, M., Wang, S., Barifcani, A., & Iglauer, S. (2017b). Stabilising nanofluids in saline environments. *Journal of Colloid and Interface Science*, 508, 222-229.
- Al-Anssari, S., Arif, M., Wang, S., Barifcani, A., Lebedev, M., & Iglauer, S. (2017c). Wettability of nano-treated calcite/CO₂/brine systems: Implication for enhanced CO₂ storage potential. *International Journal of Greenhouse Gas Control*, 66, 97-105.
- Al-Anssari, S., Arif, M., Wang, S., Barifcani, A., Lebedev, M., & Iglauer, S. (2018). Wettability of nanofluid-modified oil-wet calcite at reservoir conditions. *Fuel*, 211, 405-414.
- Al-Khdheawi, E. A., Vialle, S., Barifcani, A., Sarmadivaleh, M., & Iglauer, S. (2017a). Effect of brine salinity on CO₂ plume migration and trapping capacity in deep saline aquifers. *The APPEA Journal*, 57(1), 100-109.
- Al-Khdheawi, E. A., Vialle, S., Barifcani, A., Sarmadivaleh, M., & Iglauer, S. (2017b). Influence of injection well configuration and rock wettability on CO₂ plume behaviour and CO₂ trapping capacity in heterogeneous reservoirs. *Journal of Natural Gas Science and Engineering*, 43, 190-206.
- Al-Menhali, A. S., Menke, H. P., Blunt, M. J., & Krevor, S. C. (2016). Pore scale observations of trapped CO₂ in mixed-wet carbonate rock: applications to storage in oil fields. *Environmental Science & Technology*, 50(18), 10282-10290.
- Al-Yaseri, A. Z., Lebedev, M., Barifcani, A., & Iglauer, S. (2016). Receding and advancing (CO₂+ brine+ quartz) contact angles as a function of pressure, temperature, surface roughness, salt type and salinity. *The Journal of Chemical Thermodynamics*, 93, 416-423.

- Alroudhan, A., Vinogradov, J., & Jackson, M. D. (2016). Zeta potential of intact natural limestone: Impact of potential-determining ions Ca, Mg and SO₄. *Colloids and Surfaces A: Physicochemical and Engineering Aspects*, 493, 83-98.
- Amaya, J., Rana, D., & Hornof, V. (2002). Dynamic interfacial tension behavior of water/oil systems containing in situ-formed surfactants. *Journal of Solution Chemistry*, 31(2), 139-148.
- Amott, E. (1959). Observations relating to the wettability of porous rock.
- Anderson, W. G. (1986). Wettability literature survey-part 1: Rock/oil/brine interactions and the effects of core handling on wettability. *Journal of Petroleum Technology*, 38(10), 1-125.
- Arif, M., Al-Yaseri, A. Z., Barifcani, A., Lebedev, M., & Iglauer, S. (2016a). Impact of pressure and temperature on CO₂-brine-mica contact angles and CO₂-brine interfacial tension: Implications for carbon geo-sequestration. *Journal of Colloid and Interface Science*, 462, 208-215.
- Arif, M., Barifcani, A., Lebedev, M., & Iglauer, S. (2016b). Structural trapping capacity of oil-wet caprock as a function of pressure, temperature and salinity. *International Journal of Greenhouse Gas Control*, 50, 112-120.
- Arif, M., Barifcani, A., Lebedev, M., & Iglauer, S. (2016c). CO₂-wettability of low to high rank coal seams: Implications for carbon sequestration and enhanced methane recovery. *Fuel*, 181, 680-689.
- Arif, M., Barifcani, A., & Iglauer, S. (2016d). Solid/CO₂ and solid/water interfacial tensions as a function of pressure, temperature, salinity and mineral type: Implications for CO₂-wettability and CO₂ geo-storage. *International Journal of Greenhouse Gas Control*, 53, 263-273.
- Arif, M., Barifcani, A., Lebedev, M., & Iglauer, S. (2016e). CO₂ Wettability of Shales and Coals as a Function of Pressure, Temperature and Rank: Implications for CO₂ Sequestration and Enhanced Methane Recovery. In *PAPG/SPE Pakistan Section Annual Technical Conference and Exhibition*. Society of Petroleum Engineers.
- Arif, M. (2017). *Experimental Investigation of Wettability of Rock-CO₂-Brine for Improved Reservoir Characterization*. Doctoral dissertation, Curtin University.
- Arif, M., Lebedev, M., Barifcani, A., & Iglauer, S. (2017a). CO₂ storage in carbonates: Wettability of calcite. *International Journal of Greenhouse Gas Control*, 62, 113-121.

- Arif, M., Lebedev, M., Barifcani, A., & Iglauer, S. (2017b), Influence of shale-total organic content on CO₂ geo-storage potential. *Geophysical Research Letters*.doi:10.1002/2017GL073532.
- Arif, M., Jones, F., Barifcani, A., & Iglauer, S. (2017c). Influence of surface chemistry on interfacial properties of low to high rank coal seams. *Fuel*, 194, 211-221.
- Arif, M., Jones, F., Barifcani, A., & Iglauer, S. (2017d). Electrochemical investigation of the effect of temperature, salinity and salt type on brine/mineral interfacial properties. *International Journal of Greenhouse Gas Control*, 59, 136-147.
- Arif, M., Barifcani, A., Lebedev, M., & Iglauer, S. (2017e). Impact of Solid Surface Energy on Wettability of CO₂-brine-Mineral Systems as a Function of Pressure, Temperature and Salinity. *Energy Procedia*, 114, 4832-4842.
- Bachu, S., Gunter, W. D., & Perkins, E. H. (1994). Aquifer disposal of CO₂: hydrodynamic and mineral trapping. *Energy Conversion and Management*, 35(4), 269-279.
- Barth, T. (1991). Organic acids and inorganic ions in waters from petroleum reservoirs, Norwegian continental shelf: A multivariate statistical analysis and comparison with American reservoir formation waters. *Applied Geochemistry*, 6(1), 1-15.
- Bennett, P. C., Siegel, D. E., Baedeker, M. J., & Hult, M. F. (1993). Crude oil in a shallow sand and gravel aquifer—I. Hydrogeology and inorganic geochemistry. *Applied Geochemistry*, 8(6), 529-549.
- Benson, S. M., & Orr, F. M. (2008). Carbon dioxide capture and storage. *Mrs Bulletin*, 33(4), 303-305.
- Bhown, A. S., & Freeman, B. C. (2011). Analysis and status of post-combustion carbon dioxide capture technologies. *Environmental Science & Technology*, 45(20), 8624-8632.
- Bickle, M. J. (2009). Geological carbon storage. *Nature Geoscience*, 2(12), 815-818.
- Birkholzer, J. T., Zhou, Q., & Tsang, C. F. (2009). Large-scale impact of CO₂ storage in deep saline aquifers: a sensitivity study on pressure response in stratified systems. *International Journal of Greenhouse Gas Control*, 3(2), 181-194.
- Broseta, D., Tonnet, N., & Shah, V. (2012). Are rocks still water-wet in the presence of dense CO₂ or H₂S? *Geofluids*, 12(4), 280-294.
- Bryant, S., & Blunt, M. (1992). Prediction of relative permeability in simple porous media. *Physical Review A*, 46(4), 2004.

- Budisa, N., & Schulze-Makuch, D. (2014). Supercritical carbon dioxide and its potential as a life-sustaining solvent in a planetary environment. *Life*, 4(3), 331-340.
- Burnside, N., & Naylor, M. (2011) Evaluation of CO₂ storage actuarial risk: Defining an evidence base. DEVEX, 12th May, *School of Geoscience, University of Edinburgh, Aberdeen*.
- Cao, Z., Daly, M., Clémence, L., Geever, L. M., Major, I., Higginbotham, C. L., & Devine, D. M. (2016). Chemical surface modification of calcium carbonate particles with stearic acid using different treating methods. *Applied Surface Science*, 378, 320-329.
- Cape Grim (2017). *Cape Grim Greenhouse Gas Web Data*. <http://www.csiro.au/greenhouse-gases/>.
- Chaudhary, K., Gultinan, E. J., Cardenas, M. B., Maisano, J. A., Ketcham, R. A., & Bennett, P. C. (2015). Wettability measurement under high P-T conditions using X-ray imaging with application to the brine-supercritical CO₂ system. *Geochemistry, Geophysics, Geosystems*, 16(9), 2858-2864.
- Chaudhary, K., Bayani Cardenas, M., Wolfe, W. W., Maisano, J. A., Ketcham, R. A., & Bennett, P. C. (2013). Pore-scale trapping of supercritical CO₂ and the role of grain wettability and shape. *Geophysical Research Letters*, 40(15), 3878-3882.
- Change, I. C. (2007). Mitigation of climate change. *Summary for Policymakers*, 10(5.4).
- Chen, C., Wan, J., Li, W., & Song, Y. (2015). Water contact angles on quartz surfaces under supercritical CO₂ sequestration conditions: Experimental and molecular dynamics simulation studies. *International Journal of Greenhouse Gas Control*, 42, 655-665.
- Chiquet, P., Broseta, D., & Thibeau, S. (2007). Wettability alteration of caprock minerals by carbon dioxide. *Geofluids*, 7(2), 112-122.
- Chu, S., & Majumdar, A. (2012). Opportunities and challenges for a sustainable energy future. *Nature*, 488(7411), 294.
- Class, H., Ebigbo, A., Helmig, R., Dahle, H. K., Nordbotten, J. M., Celia, M. A., ...& Flemisch, B. (2009). A benchmark study on problems related to CO₂ storage in geologic formations. *Computational Geosciences*, 13(4), 409.
- CO₂CRC web data, retrieved from: www.co2crc.com.au
- Cyr, T. D., & Strausz, O. P. (1984). Bound carboxylic acids in the Alberta oil sands. *Organic Geochemistry*, 7(2), 127-140.
- Davis, S. J., Caldeira, K., & Matthews, H. D. (2010). Future CO₂ emissions and climate change from existing energy infrastructure. *Science*, 329(5997), 1330-1333.

- Davis, S. C., Williams, S. E., & Boundy, R. G. (2016). *Transportation Energy Data Book: Edition 35* (No. ORNL/TM-2016/470). Oak Ridge National Laboratory (ORNL), Oak Ridge, TN (United States).
- Dickson, J. L., Gupta, G., Horozov, T. S., Binks, B. P., & Johnston, K. P. (2006). Wetting phenomena at the CO₂/water/glass interface. *Langmuir*, 22(5), 2161-2170.
- Donaldson, E. C., Thomas, R. D., & Lorenz, P. B. (1969). Wettability determination and its effect on recovery efficiency. *Society of Petroleum Engineers Journal*, 9(01), 13-20.
- El-Maghraby, R. M., & Blunt, M. J. (2012). Residual CO₂ trapping in Indiana limestone. *Environmental Science & Technology*, 47(1), 227-233.
- Eral, H. B., & Oh, J. M. (2013). Contact angle hysteresis: A review of fundamentals and applications. *Colloid and Polymer Science*, 291(2), 247-260.
- Farokhpoor, R., Bjørkvik, B. J., Lindeberg, E., & Torsæter, O. (2013). Wettability behaviour of CO₂ at storage conditions. *International Journal of Greenhouse Gas Control*, 12, 18-25.
- Feng, L., Wang, W., Cheng, J., Ren, Y., Zhao, G., Gao, C., ...& Liu, R. (2007). Genome and proteome of long-chain alkane degrading *Geobacillus thermodenitrificans* NG80-2 isolated from a deep-subsurface oil reservoir. *Proceedings of the National Academy of Sciences*, 104(13), 5602-5607.
- Fiala, N. (2009). The greenhouse hamburger. *Scientific American*, 300(2), 72-75.
- Froelich, P., Klinkhammer, G. P., Bender, M. L., Luedtke, N. A., Heath, G. R., Cullen, D., ... & Maynard, V. (1979). Early oxidation of organic matter in pelagic sediments of the eastern equatorial Atlantic: Suboxic diagenesis. *Geochimica et Cosmochimica Acta*, 43(7), 1075-1090.
- Golding, S. D., Uysal, I. T., Boreham, C. J., Kirste, D., Baublys, K. A., & Esterle, J. S. (2011). Adsorption and mineral trapping dominate CO₂ storage in coal systems. *Energy Procedia*, 4, 3131-3138.
- Gomari, K. R., & Hamouda, A. A. (2006). Effect of fatty acids, water composition and pH on the wettability alteration of calcite surface. *Journal of Petroleum Science and Engineering*, 50(2), 140-150.
- Gomari, K. R., Hamouda, A. A., Davidian, T., & Fargland, D. A. (2006). Study of the effect of acidic species on wettability alteration of calcite surfaces by measuring partitioning coefficients, IFT and contact angles. *Contact Angle, Wettability and Adhesion*, 4, 351-367.

- Grabowski, A., Blanchet, D., & Jeanthon, C. (2005). Characterization of long-chain fatty-acid-degrading syntrophic associations from a biodegraded oil reservoir. *Research in Microbiology*, 156(7), 814-821.
- GRREBS (French energy research group) web data. Retrieved from: http://grrebs.ete.inrs.ca/en/csc/csc_stockage/
- Guiltinan, E. J., Cardenas, M. B., Bennett, P. C., Zhang, T., & Espinoza, D. N. (2017). The effect of organic matter and thermal maturity on the wettability of supercritical CO₂ on organic shales. *International Journal of Greenhouse Gas Control*, 65, 15-22.
- Hamouda, A. A., & RezaeiGomari, K. A. (2006, January). Influence of temperature on wettability alteration of carbonate reservoirs. In *SPE/DOE Symposium on Improved Oil Recovery*. Society of Petroleum Engineers.
- Hansen, G., Hamouda, A. A., & Denoyel, R. (2000). The effect of pressure on contact angles and wettability in the mica/water/n-decane system and the calcite+ stearic acid/water/n-decane system. *Colloids and Surfaces A: Physicochemical and Engineering Aspects*, 172(1), 7-16.
- Harvey, O. R., Qafoku, N. P., Cantrell, K. J., Lee, G., Amonette, J. E., & Brown, C. F. (2012). Geochemical implications of gas leakage associated with geologic CO₂ storage: A qualitative review. *Environmental Science & Technology*, 47(1), 23-36.
- Haynes, W. M. (Ed.). (2014). *CRC handbook of Chemistry and Physics*. CRC press.
- Heberling, F., Trainor, T. P., Lützenkirchen, J., Eng, P., Denecke, M. A., & Bosbach, D. (2011). Structure and reactivity of the calcite–water interface. *Journal of Colloid and Interface Science*, 354(2), 843-857.
- Herrero, M., Henderson, B., Havlík, P., Thornton, P. K., Conant, R. T., Smith, P., ...& Butterbach-Bahl, K. (2016). Greenhouse gas mitigation potentials in the livestock sector. *Nature Climate Change*.
- Hoeiland, S., Barth, T., Blokhus, A. M., & Skauge, A. (2001). The effect of crude oil acid fractions on wettability as studied by interfacial tension and contact angles. *Journal of Petroleum Science and Engineering*, 30(2), 91-103.
- Holloway, S. (2007). Carbon dioxide capture and geological storage. *Philosophical Transactions of the Royal Society of London A: Mathematical, Physical and Engineering Sciences*, 365(1853), 1095-1107.
- Hristov, A. N., Oh, J., Lee, C., Meinen, R., Montes, F., Ott, T., ...& Yang, W. (2013). Mitigation of greenhouse gas emissions in livestock production: A review of technical

- options for non-CO₂ emissions. *FAO Animal Production and Health Paper No, 177*, 1-206.
- Hurlbut, C. S., & Klein, C., 1985, *Manual of Mineralogy*, 20th ed., Wiley, ISBN 0-471-80580-7.
- Iglauer, S., Paluszny, A., Pentland, C. H., & Blunt, M. J. (2011a). Residual CO₂ imaged with X-ray micro-tomography. *Geophysical Research Letters*, 38 (21).
- Iglauer, S., Wüiling, W., Pentland, C. H., Al-Mansoori, S. K., & Blunt, M. J. (2011b). Capillary-trapping capacity of sandstones and sandpacks. *SPE Journal*, 16(4), 778-783.
- Iglauer, S. (2011c). *Dissolution trapping of carbon dioxide in reservoir formation brine-a carbon storage mechanism*. INTECH Open Access Publisher.
- Iglauer, S., Mathew, M. S., & Bresme, F. (2012). Molecular dynamics computations of brine–CO₂ interfacial tensions and brine–CO₂–quartz contact angles and their effects on structural and residual trapping mechanisms in carbon geo-sequestration. *Journal of Colloid and Interface Science*, 386(1), 405-414.
- Iglauer, S., Paluszny, A., & Blunt, M. J. (2013). Simultaneous oil recovery and residual gas storage: A pore-level analysis using in situ X-ray micro-tomography. *Fuel*, 103, 905-914.
- Iglauer, S., Salamah, A., Sarmadivaleh, M., Liu, K., & Phan, C. (2014). Contamination of silica surfaces: Impact on water–CO₂–quartz and glass contact angle measurements. *International Journal of Greenhouse Gas Control*, 22, 325-328.
- Iglauer, S., Pentland, C. H., & Busch, A. (2015a). CO₂ wettability of seal and reservoir rocks and the implications for carbon geo-sequestration. *Water Resources Research*, 51(1), 729-774.
- Iglauer, S., Al-Yaseri, A. Z., Rezaee, R., & Lebedev, M. (2015b). CO₂ wettability of caprocks: Implications for structural storage capacity and containment security. *Geophysical Research Letters*, 42(21), 9279-9284.
- Iglauer, S. (2017). CO₂–Water–Rock Wettability: Variability, Influencing Factors, and Implications for CO₂ geo-storage. *Accounts of Chemical Research*, 50(5), 1134-1142.
- IPCC. (2005). Carbon dioxide capture and storage. In: B. Metz, O. Davidson, H.d. Coninck, M. Loos, L. Meyer (Eds.) *IPCC*, 2005.
- Jackson, M. D., Al-Mahrouqi, D., & Vinogradov, J. (2016). Zeta potential in oil-water-carbonate systems and its impact on oil recovery during controlled salinity water-flooding. *Scientific Reports*, 6.

- Jardine, P. M., McCarthy, J. F., & Weber, N. L. (1989). Mechanisms of dissolved organic carbon adsorption on soil. *Soil Science Society of America Journal*, 53(5), 1378-1385.
- Ji, X., & Zhu, C. (2015). CO₂ storage in deep saline aquifers. Chapter 10 in *Novel Mater, Carbon Dioxide Mitigation Technology*, 299-332.
- Jones, D. M., Head, I. M., Gray, N. D., Adams, J. J., Rowan, A. K., Aitken, C. M., ...& Oldenburg, T. (2008). Crude-oil biodegradation via methanogenesis in subsurface petroleum reservoirs. *Nature*, 451(7175), 176.
- Juanes, R., MacMinn, C. W., & Szulczewski, M. L. (2010). The footprint of the CO₂ plume during carbon dioxide storage in saline aquifers: storage efficiency for capillary trapping at the basin scale. *Transport in Porous Media*, 82(1), 19-30.
- Karl, T. R. (Ed.). (2009). *Global climate change impacts in the United States*. Cambridge University Press.
- Karoussi, O., Skovbjerg, L. L., Hassenkam, T., Stipp, S. S., & Hamouda, A. A. (2008). AFM study of calcite surface exposed to stearic and heptanoic acids. *Colloids and Surfaces A: Physicochemical and Engineering Aspects*, 325(3), 107-114.
- Kelemen, P. B., & Matter, J. (2008). In situ carbonation of peridotite for CO₂ storage. *Proceedings of the National Academy of Sciences*, 105(45), 17295-17300.
- Kharaka, Y. K., Thordsen, J. J., Hovorka, S. D., Nance, H. S., Cole, D. R., Phelps, T. J., & Knauss, K. G. (2009). Potential environmental issues of CO₂ storage in deep saline aquifers: Geochemical results from the Frio-I Brine Pilot test, Texas, USA. *Applied Geochemistry*, 24(6), 1106-1112.
- King, M. B., & Bott, T. R. (Eds.). (2012). *Extraction of natural products using near-critical solvents*. Springer Science & Business Media.
- Kovscek, A. R. (2002). Screening criteria for CO₂ storage in oil reservoirs. *Petroleum Science and Technology*, 20(7-8), 841-866.
- Krevor, S., Pini, R., Zuo, L., & Benson, S. M. (2012). Relative permeability and trapping of CO₂ and water in sandstone rocks at reservoir conditions. *Water Resources Research*, 48(2).
- Krevor, S., Blunt, M. J., Benson, S. M., Pentland, C. H., Reynolds, C., Al-Menhali, A., & Niu, B. (2015). Capillary trapping for geologic carbon dioxide storage—From pore scale physics to field scale implications. *International Journal of Greenhouse Gas Control*, 40, 221-237.

- Kumar, A., Noh, M. H., Ozah, R. C., Pope, G. A., Bryant, S. L., Sepehrnoori, K., & Lake, L. W. (2005). Reservoir simulation of CO₂ storage in aquifers. *SPE Journal*, *10*(03), 336-348.
- Kvenvolden, K. A. (1967). Normal fatty acids in sediments. *Journal of the American Oil Chemists' Society*, *44*(11), 628-636.
- Lackner, K. S. (2003). A guide to CO₂ sequestration. *Science*, *300*(5626), 1677-1678.
- Lander, L. M., Siewierski, L. M., Brittain, W. J., & Vogler, E. A. (1993). A systematic comparison of contact angle methods. *Langmuir*, *9*, 2237-2237.
- Legens, C., Toulhoat, H., Cuiec, L., Villieras, F., & Palermo, T. (1998, January). Wettability change related to the adsorption of organic acids on calcite: Experimental and ab initio computational studies. In *SPE Annual Technical Conference and Exhibition*. Society of Petroleum Engineers.
- Love, J. C., Estroff, L. A., Kriebel, J. K., Nuzzo, R. G., & Whitesides, G. M. (2005). Self-assembled monolayers of thiolates on metals as a form of nanotechnology. *Chemical reviews*, *105*(4), 1103-1170.
- Madsen, L., & Ida, L. (1998). Adsorption of carboxylic acids on reservoir minerals from organic and aqueous phase. *SPE Reservoir Evaluation & Engineering*, *1*(01), 47-51.
- Markewitz, P., & Bongartz, R. (2015). Carbon capture technologies. In *Carbon Capture, Storage and Use* (pp. 13-45). Springer International Publishing.
- McGowan, C. W., Pearce, R. C., & Diehl, H. (1985). A comparison of the dissolution of model compounds and the kerogen of Green River oil shale by oxidation with perchloric acid—A model for the kerogen of Green River oil shale. *Fuel Processing Technology*, *10*(2), 195-204.
- Meredith, W., Kelland, S. J., & Jones, D. M. (2000). Influence of biodegradation on crude oil acidity and carboxylic acid composition. *Organic Geochemistry*, *31*(11), 1059-1073.
- Mihajlović, S. R., Vučinić, D. R., Sekulić, Ž. T., Milićević, S. Z., & Kolonja, B. M. (2013). Mechanism of stearic acid adsorption to calcite. *Powder Technology*, *245*, 208-216.
- Morrow, N. R. (1970). Physics and thermodynamics of capillary action in porous media. *Industrial & Engineering Chemistry*, *62*(6), 32-56.
- Morrow, N. R. (1990). Wettability and its effect on oil recovery. *Journal of Petroleum Technology*, *42*(12), 1-476.
- Naylor, M., Wilkinson, M., & Haszeldine, R. S. (2011). Calculation of CO₂ column heights in depleted gas fields from known pre-production gas column heights. *Marine and Petroleum Geology*, *28*(5), 1083-1093.

- Nordbotten, J. M., Celia, M. A., & Bachu, S. (2005). Injection and storage of CO₂ in deep saline aquifers: analytical solution for CO₂ plume evolution during injection. *Transport in Porous Media*, 58(3), 339-360.
- Nordhaus, W. D. (2014). *A question of balance: Weighing the options on global warming policies*. Yale University Press.
- Pearce, J. K., Kirste, D. M., Dawson, G. K., Farquhar, S. M., Biddle, D., Golding, S. D., & Rudolph, V. (2015). SO₂ impurity impacts on experimental and simulated CO₂-water-reservoir rock reactions at carbon storage conditions. *Chemical Geology*, 399, 65-86.
- Pentland, C. H., El-Maghraby, R., Georgiadis, A., Iglauer, S., & Blunt, M. J. (2011). Immiscible displacements and capillary trapping in CO₂ storage. *Energy Procedia*, 4, 4969-4976.
- Pires, J. C. M., Martins, F. G., Alvim-Ferraz, M. C. M., & Simões, M. (2011). Recent developments on carbon capture and storage: an overview. *Chemical Engineering Research and Design*, 89(9), 1446-1460.
- Posch, S., & Haider, M. (2012). Optimization of CO₂ compression and purification units (CO₂ CPU) for CCS power plants. *Fuel*, 101, 254-263.
- Qi, R., LaForce, T. C., & Blunt, M. J. (2009). Design of carbon dioxide storage in aquifers. *International Journal of Greenhouse Gas Control*, 3(2), 195-205.
- Rackley, S. A. (2009). *Carbon capture and storage*. Gulf Professional Publishing.
- Rahman, T., Lebedev, M., Barifcani, A., & Iglauer, S. (2016). Residual trapping of supercritical CO₂ in oil-wet sandstone. *Journal of Colloid and Interface Science*, 469, 63-68.
- Rosenberg, N. J. (1981). The increasing CO₂ concentration in the atmosphere and its implication on agricultural productivity. *Climatic Change*, 3(3), 265-279.
- Roshan, H., Al-Yaseri, A. Z., Sarmadivaleh, M., & Iglauer, S. (2016). On wettability of shale rocks. *Journal of Colloid and Interface Science*, 475, 104-111.
- Saadatpoor, E., Bryant, S. L., & Sepehrnoori, K. (2010). New trapping mechanism in carbon sequestration. *Transport in Porous Media*, 82(1), 3-17.
- Saghafi, A., Javanmard, H., & Pinetown, K. (2014). Study of coal gas wettability for CO₂ storage and CH₄ recovery. *Geofluids*, 14(3), 310-325.
- Saraji, S., L. Goual, M. Piri, & H. Plancher (2013), Wettability of supercritical carbon dioxide/water/quartz systems: Simultaneous measurement of contact angle and interfacial tension at reservoir conditions, *Langmuir*, 29, 6856-6866.

- Sarmadivaleh, M., Al-Yaseri, A. Z., & Iglauer, S. (2015). Influence of temperature and pressure on quartz–water–CO₂ contact angle and CO₂–water interfacial tension. *Journal of Colloid and Interface Science*, *441*, 59-64.
- Schiermeier, Q., Tollefson, J., Scully, T., Witze, A., & Morton, O. (2008). Energy alternatives: Electricity without carbon. *Nature News*, *454*(7206), 816-823.
- Seewald, J. S. (2003). Organic-inorganic interactions in petroleum-producing sedimentary basins. *Nature*, *426*(6964), 327.
- Shi, X., Rosa, R., & Lazzeri, A. (2010). On the coating of precipitated calcium carbonate with stearic acid in aqueous medium. *Langmuir*, *26*(11), 8474-8482.
- ShojaiKaveh, N., Rudolph, E. S. J., Wolf, K. H. A., & Ashrafizadeh, S. N. (2011). Wettability determination by contact angle measurements: hvBb coal–water system with injection of synthetic flue gas and CO₂. *Journal of Colloid and Interface Science*, *364*(1), 237-247.
- ShojaiKaveh, N., Wolf, K. H., Ashrafizadeh, S. N., & Rudolph, E. S. J. (2012). Effect of coal petrology and pressure on wetting properties of wet coal for CO₂ and flue gas storage. *International Journal of Greenhouse Gas Control*, *11*, S91-S101.
- ShojaiKaveh, N., Barnhoorn, A., & Wolf, K. H. (2016). Wettability evaluation of silty shale caprocks for CO₂ storage. *International Journal of Greenhouse Gas Control*, *49*, 425-435.
- Solomon, S., Plattner, G. K., Knutti, R., & Friedlingstein, P. (2009). Irreversible climate change due to carbon dioxide emissions. *Proceedings of the National Academy of Sciences*, *106*(6), 1704-1709.
- Speight, J. G. (2005). *Lange's handbook of Chemistry* (Vol. 1). New York: McGraw-Hill.
- Spiteri, E. J., Juanes, R., Blunt, M. J., & Orr, F. M. (2008). A new model of trapping and relative permeability hysteresis for all wettability characteristics. *SPE Journal*, *13*(03), 277-288.
- Stalker, L., Varma, S., Van Gent, D., Haworth, J., & Sharma, S. (2013). South West Hub: A carbon capture and storage project. *Australian Journal of Earth Sciences*, *60*(1), 45-58.
- Standnes, D. C., & Austad, T. (2003). Wettability alteration in carbonates: Interaction between cationic surfactant and carboxylates as a key factor in wettability alteration from oil-wet to water-wet conditions. *Colloids and Surfaces A: Physicochemical and Engineering Aspects*, *216*(1), 243-259.

- Stipp, S. L. S., Gutmannsbauer, W., & Lehmann, T. (1996). The dynamic nature of calcite surfaces in air. *American Mineralogist*, *81*(1-2), 1-8.
- Svensson, R., Odenberger, M., Johnsson, F., & Strömberg, L. (2004). Transportation systems for CO₂—application to carbon capture and storage. *Energy Conversion and Management*, *45*(15), 2343-2353.
- Tabrizy, V. A., Denoyel, R., & Hamouda, A. A. (2011). Characterization of wettability alteration of calcite, quartz and kaolinite: Surface energy analysis. *Colloids and Surfaces A: Physicochemical and Engineering Aspects*, *384*(1), 98-108.
- Thomas, D. C., & Benson, S. M. (Eds.). (2015). *Carbon dioxide capture for storage in deep geologic formations-results from the CO₂ Capture Project: Vol 2-Geologic Storage of Carbon Dioxide with Monitoring and Verification*. Elsevier.
- Thurman, E. M. (1985). Amino acids. In *Organic geochemistry of natural waters* (pp. 151-180). Springer Netherlands.
- Townsend, G. T., Prince, R. C., & Suflita, J. M. (2003). Anaerobic oxidation of crude oil hydrocarbons by the resident microorganisms of a contaminated anoxic aquifer. *Environmental Science & Technology*, *37*(22), 5213-5218.
- Vinogradov, J., & Jackson, M. D. (2015). Zeta potential in intact natural sandstones at elevated temperatures. *Geophysical Research Letters*, *42*(15), 6287-6294.
- Wan, J., Kim, Y., & Tokunaga, T. K. (2014). Contact angle measurement ambiguity in supercritical CO₂–water–mineral systems: Mica as an example. *International Journal of Greenhouse Gas Control*, *31*, 128-137.
- Wang, C., Sheng, Y., Zhao, X., Pan, Y., & Wang, Z. (2006). Synthesis of hydrophobic CaCO₃ nanoparticles. *Materials Letters*, *60*(6), 854-857.
- Waples, D. W. (1981). *Organic geochemistry for exploration geologists*. Burgess Pub. Co.
- Watson, J. S., Jones, D. M., Swannell, R. P. J., & Van Duin, A. C. T. (2002). Formation of carboxylic acids during aerobic biodegradation of crude oil and evidence of microbial oxidation of hopanes. *Organic Geochemistry*, *33*(10), 1153-1169.
- White, C. M., Strazisar, B. R., Granite, E. J., Hoffman, J. S., & Pennline, H. W. (2003). Separation and capture of CO₂ from large stationary sources and sequestration in geological formations—coalbeds and deep saline aquifers. *Journal of the Air & Waste Management Association*, *53*(6), 645-715.
- Winthaegen, P., Arts, R., & Schroot, B. (2005). Monitoring subsurface CO₂ storage. *Oil & Gas Science and Technology*, *60*(3), 573-582.

- Yánez-Soto, B., Leonard, B. C., Raghunathan, V. K., Abbott, N. L., & Murphy, C. J. (2015). Effect of stratification on surface properties of corneal epithelial cells effects of Engineering corneal epithelium in Dry Eye. *Investigative Ophthalmology & Visual Science*, *56*(13), 8340-8348.
- Yang, L., Xu, T., Wei, M., Feng, G., Wang, F., & Wang, K. (2015). Dissolution of arkose in dilute acetic acid solution under conditions relevant to burial diagenesis. *Applied Geochemistry*, *54*, 65-73.
- Zhang, Z. X., Wang, G. X., Massarotto, P., & Rudolph, V. (2006). Optimization of pipeline transport for CO₂ sequestration. *Energy Conversion and Management*, *47*(6), 702-715.

“Every reasonable effort has been made to acknowledge the owner of copyright material. I would be pleased to hear from any copyright owner who has been omitted or incorrectly acknowledged”.

Appendix

Example SEM images for calcite

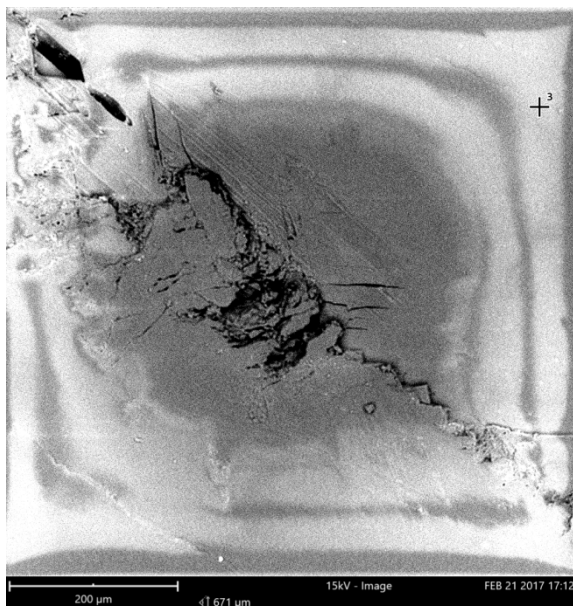


Figure: Calcite surface aged in 10⁻² M stearic acid

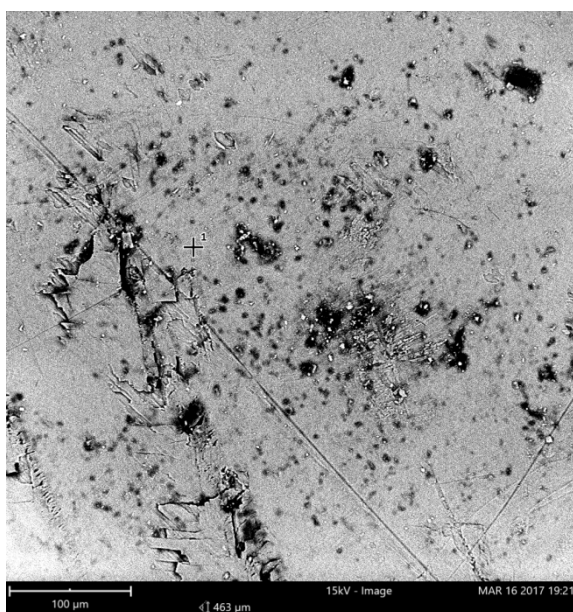


Figure: Calcite surface aged in 10⁻⁶ M stearic acid

Example SEM images for quartz

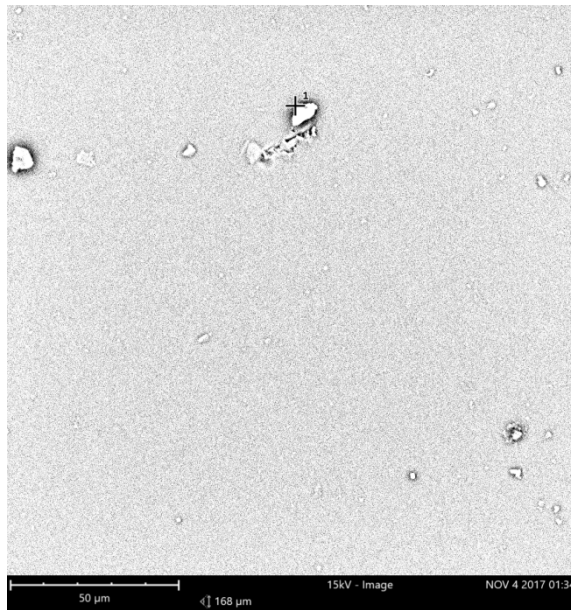


Figure: quartz surface aged in 10⁻⁴ M hexanoic acid

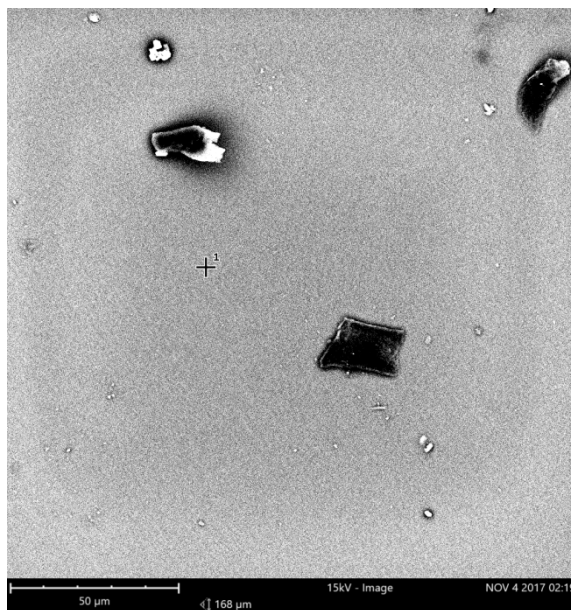


Figure: quartz surface aged in 10⁻⁴ M lauric acid

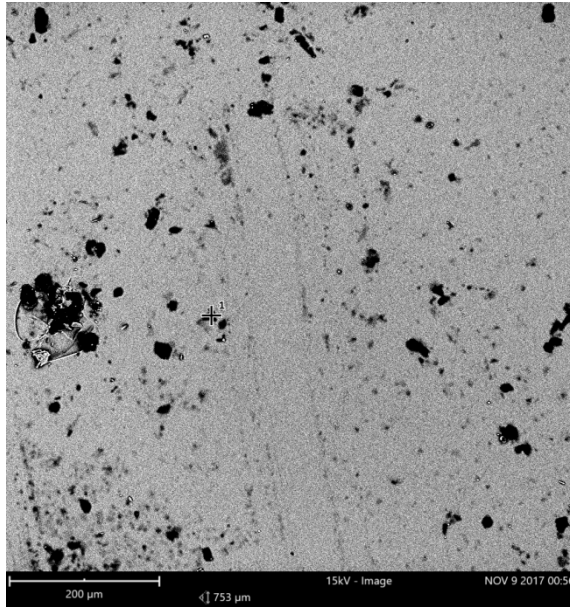


Figure: quartz surface aged in 10⁻⁴ M stearic acid

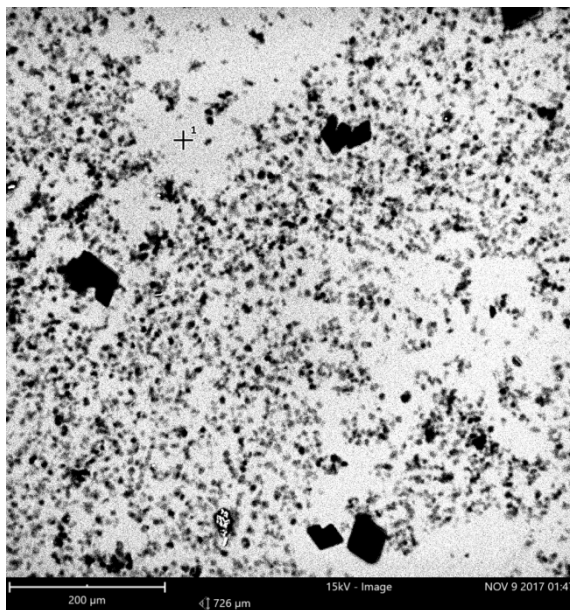


Figure: quartz surface aged in 10⁻⁴ M lignoceric acid